Design of Bandlimited, Energy Optimized Data Transmission Filter

by

Mohammed Abdul Moid

A Thesis Presented to the

FACULTY OF THE COLLEGE OF GRADUATE STUDIES

KING FAHD UNIVERSITY OF PETROLEUM & MINERALS

DHAHRAN, SAUDI ARABIA

In Partial Fulfillment of the
Requirements for the Degree of

MASTER OF SCIENCE

In

ELECTRICAL ENGINEERING

December, 1996

INFORMATION TO USERS

This manuscript has been reproduced from the microfilm master. UMI films the text directly from the original or copy submitted. Thus, some thesis and dissertation copies are in typewriter face, while others may be from any type of computer printer.

The quality of this reproduction is dependent upon the quality of the copy submitted. Broken or indistinct print, colored or poor quality illustrations and photographs, print bleedthrough, substandard margins, and improper alignment can adversely affect reproduction.

In the unlikely event that the author did not send UMI a complete manuscript and there are missing pages, these will be noted. Also, if unauthorized copyright material had to be removed, a note will indicate the deletion.

Oversize materials (e.g., maps, drawings, charts) are reproduced by sectioning the original, beginning at the upper left-hand corner and continuing from left to right in equal sections with small overlaps. Each original is also photographed in one exposure and is included in reduced form at the back of the book.

Photographs included in the original manuscript have been reproduced xerographically in this copy. Higher quality 6" x 9" black and white photographic prints are available for any photographs or illustrations appearing in this copy for an additional charge. Contact UMI directly to order.

UMI

A Bell & Howell Information Company
300 North Zeeb Road, Ann Arbor MI 48106-1346 USA
313/761-4700 800/521-0600

DESIGN OF BANDLIMITED, ENERGY OPTIMIZED DATA TRANSMISSION FILTER

BY

MOHAMMED ABDUL MOID

A Thesis Presented to the

FACULTY OF THE COLLEGE OF GRADUATE STUDIES

KING FAHD UNIVERSITY OF PETROLEUM & MINERALS

DHAHRAN, SAUDI ARABIA

In Partial Fulfillment of the
Requirements for the Degree of

MASTER OF SCIENCE

In

ELECTRICAL ENGINEERING

DECEMBER 1996

KING FAHD UNIVERSITY OF PETROLEUM AND MINERALS
DHAHRAN, SAUDI ARABIA

COLLEGE OF GRADUATE STUDIES

This thesis, written by **MOHAMMED ABDUL MOID** *under the direction of his Thesis Advisor and approved by his Thesis Committee, has been presented to and accepted by the Dean of the College of Graduate Studies, in partial fulfillment of the requirements for the degree of*

MASTER OF SCIENCE *in* **ELECTRICAL ENGINEERING.**

THESIS COMMITTEE

Dr. Essam E. Hassan (Chairman)

Dr. Hussein Baher (Member)

Dr. Talal Halawani (Member)

Dr. Zaki Alakhdhar (Member)

S. A. Al-Baiyat
Department Chairman

Dean, College of Graduate Studies

28-12-96
Date

DEDICATED TO

MY

PARENTS

Acknowledgments

All praise and thanks be to Almighty Allah, the Creator and Sustainer of the worlds, for His eternal help and guidance; and peace be upon his Prophet, Mohammed.

Acknowledgement is due to King Fahd University of Petroleum and Minerals for providing the facilities and financial assistance during the course of my master's program. I feel extremely fortunate to have worked in the Department of Electrical Engineering here.

I wish to express my sincere thanks to my advisor, Dr. Essam E. Hassan for his help and advice. I acknowledge him for his valuable guidance, time and support. I also wish to thank Dr. Hussein Baher and Dr. Talal Halawani for their help, encouragement and valuable suggestions in this work. My expression of thanks is also due to Dr. Zaki Al-Akhadar for his counsel and cooperation.

Last but not the least is the strong motivation and support provided by the whole research assistant community at KFUPM. Their cooperation has made my stay at KFUPM a memorable and pleasant one.

Contents

List of Figures

List of Tables

Abstract

Name : Mohammed Abdul Moid

Title : Design of Band Limited, Energy Optimized Data Transmission Filter.

Major Field : Electrical Engineering

Date of Degree : December 1996

A solution to the problem of designing a linear phase, Nyquist data transmission filter with rapidly decaying impulse response beyond the main lobe is attempted. Based on a recent contribution [1], the proposed technique utilizes its filter model to maximize the ratio of the energy within a specific time duration to the total energy under the full bandwidth. The denominator of the transfer functions is the linear phase polynomial and the design involves the determination of the numerator coefficients to meet the required specifications. The signal shapes thus obtained are useful in combating intersymbol interference and are almost immune to jitter effects at the receiver.

Master of Science Degree

King Fahd University of Petroleum and Minerals

Dhahran, Saudi Arabia

خلاصة الرسالة

اسم الطالب الكامل : محمد عبد المعيد

عنوان الدراسة : تصميم مرشح نقل المعلومات ذوالطيف المحددوالطاقةالمحسنة

التخصص : هندسة كهربائية

تاريخ الشهادة : نوفمبر ١٩٩٦

هذاالبحث يحتوي على محاولة لإيجاد حل لمشكلة تصميم مرشح نقل المعلومات « نكوست » مستقيم الطور وذو خاصية الانحدار السريع بعد المغزل الرئيسي . ومن منطلق الاسهام الحديث . فالطريقة المقدمة تستخدم نموذج المرشح المذكور في {١} لزيادة نسبة الطاقة المبعوثة خلال وقت محدد إلى الطاقة المبعوثة في الطيف الكلى .مقام دالة التحويل يتكون كثيرة الحدود ذات الطورالمستقيم والتصميم يضم تحديد معاملات البسط التي تحقق المواصفات المطلوبة . وقد وجد أن شكل الإشارة الناتجة مفيد في إلغاء التداخل بين الرموز ويخص أيضا من تأثير المشوش على المستقبل .

درجة الماجستير في العلوم
جامعة الملك فهد للبترول والمعادن
الظهران – المملكة العربية السعودية

Chapter 1

Introduction

1.1 General

At present, communication is of fundamental importance to the modern world. Communication is essentially the process of transferring information from one point in space or time called the source to another point called the user destination. Figure (1.1) shows the fundamental block diagram of a baseband binary data transmission system. The input to the system is a binary data sequence at a bit rate of r_b and bit duration of T. The pulse generator output is a pulse waveform [16]

$$x(t) = \sum_{k=-\infty}^{\infty} a_k p_g(t - kT) \tag{1.1}$$

where $p_g(t)$ is the basic pulse whose amplitude a_k depends on the k^{th} input bit.

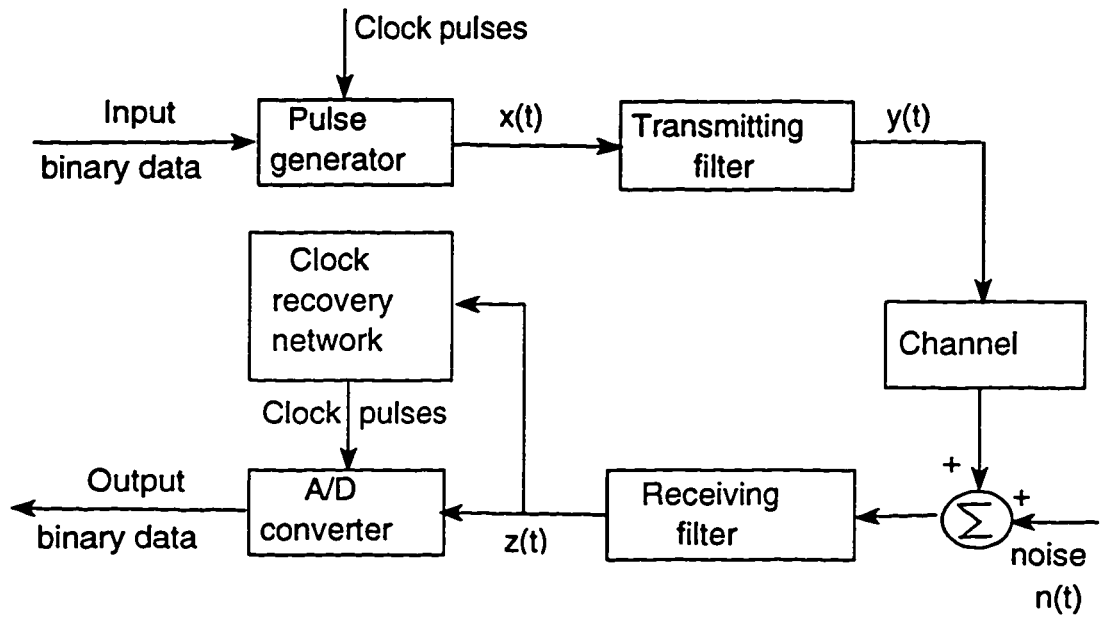

Figure 1.1: A binary data transmission system [16].

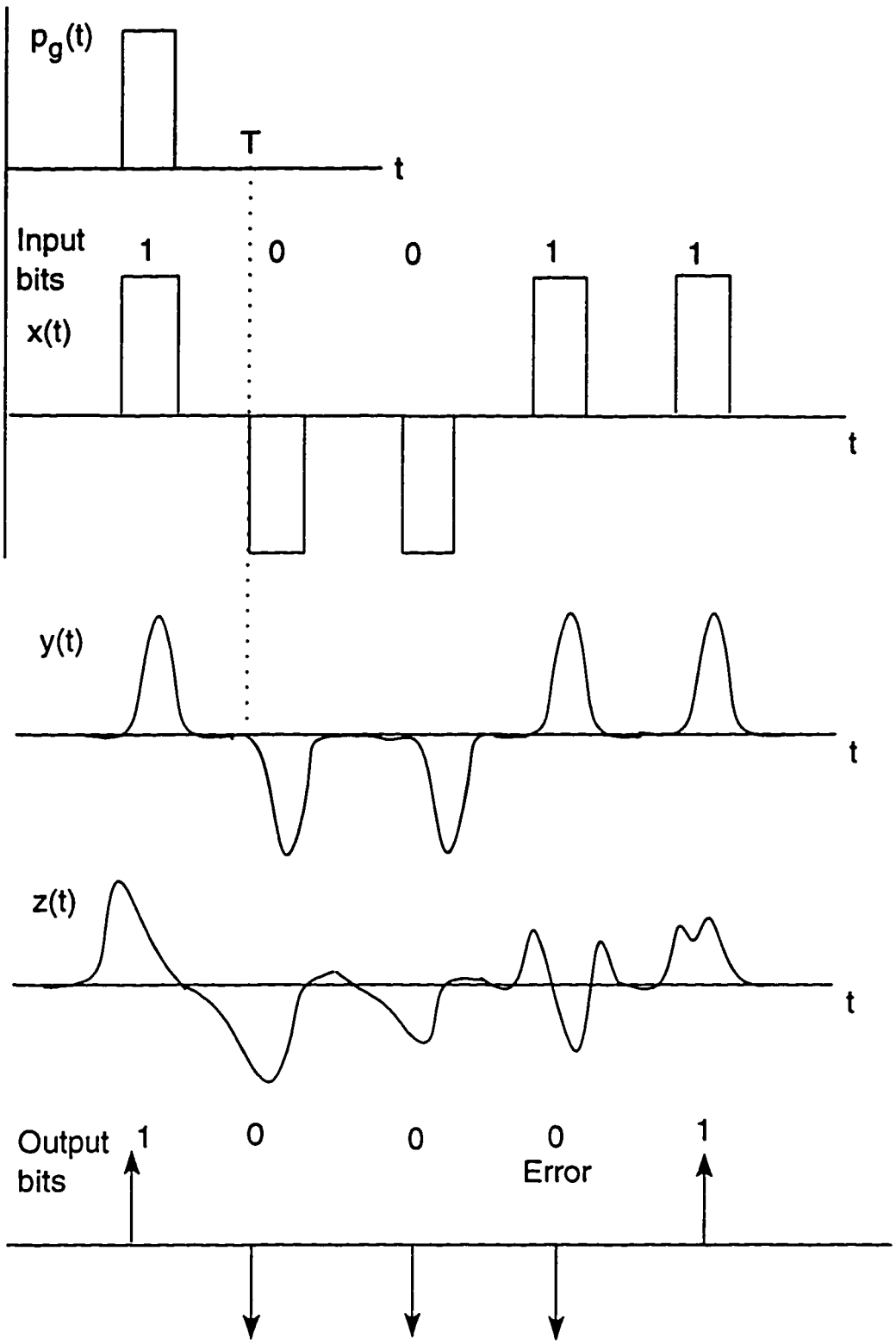

Figure 1.2: Typical waveforms of a binary data transmission system [16].

Figure (1.2) shows typical waveforms at various stages of the transmission system. The signal $x(t)$ passes through a transmitting filter which is a pulse shaping network to meet the frequency specifications of the channel. The output of the transmission filter is denoted by $y(t)$. The channel adds random noise to this signal resulting in the distorted signal $z(t)$. The transmitted bit stream is regenerated at the receiver by the A/D converter based on sampled values of the received response. Depending on the level of noise, the output of the system may or may not have random errors [16].

1.2 Transmission Filter

The design of data transmission filters plays an important role in the performance of a communication system. A data transmission filter is basically a pulse (or impulse) shaping network. It has an impulse response that produces minimal interference with the time-shifted versions of itself at an infinite number of equally spaced points that are called the ideal sampling points [1]. The interference at the sampling points is called as intersymbol interference(ISI).

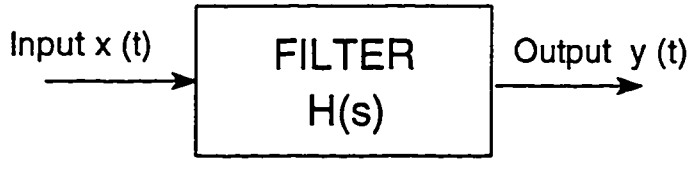

Figure 1.3: Symbolic representation of a filter

The block diagram of a filter may be represented by figure 1.3, where x(t) is the input signal, y(t) is the output signal and H(s) is the filter network transfer function. The system input and output are related as

$$Y(s) = H(s) \times X(s) \tag{1.2}$$

where $s = \sigma + jw$ is the complex frequency. The quantities Y(s) and X(s) are the Laplace transforms of y(t) and x(t) respectively. When $s = jw$ (w measured in radian/second), the network function is complex and may be written in the form

$$H(jw) = |H(jw)|e^{j\phi(w)} \tag{1.3}$$

where $|H(jw)|$ is the magnitude and $\phi(w)$ is the phase of the filter transfer function. Figures (1.4- 1.6) show the general features of the frequency, time and phase response of a data transmission filter respectively.

In a data transmission system, the information is contained in a sequence of impulses at the input to the system. Thus, a signal $x(t)$ having an amplitude of 0 or 1 is transmitted every T seconds. A sequence of input signals in general, produce a sequence of overlapping pulses at the output [7]. Figure (1.7) shows the output waveform of the transmission filter.

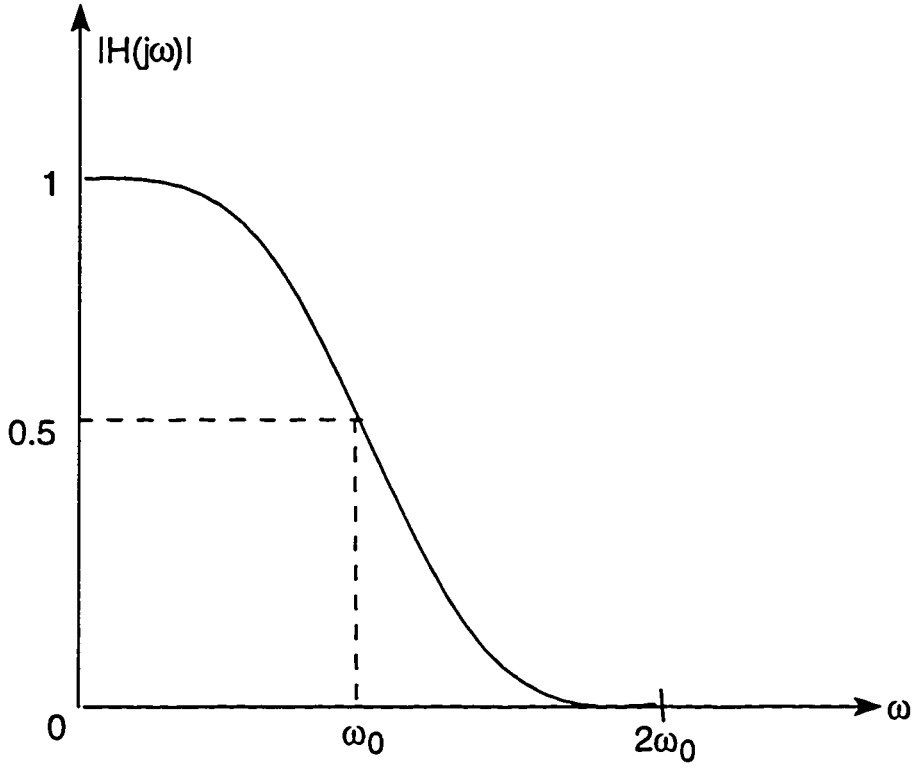

Figure 1.4: General features of expected frequency response [1]

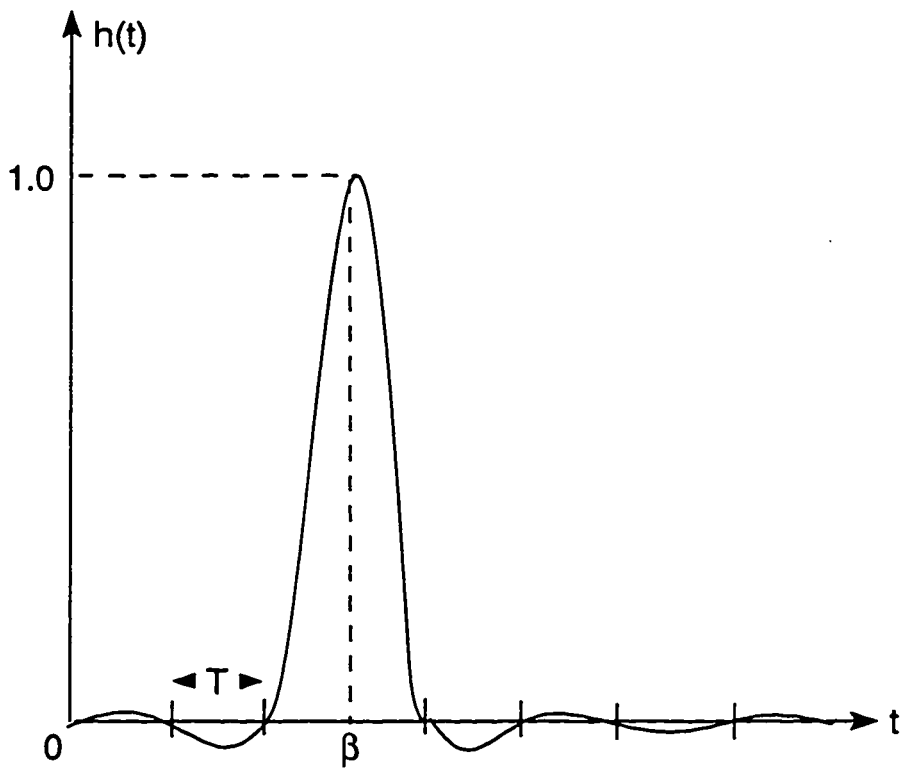

Figure 1.5: General features of expected time response [1]

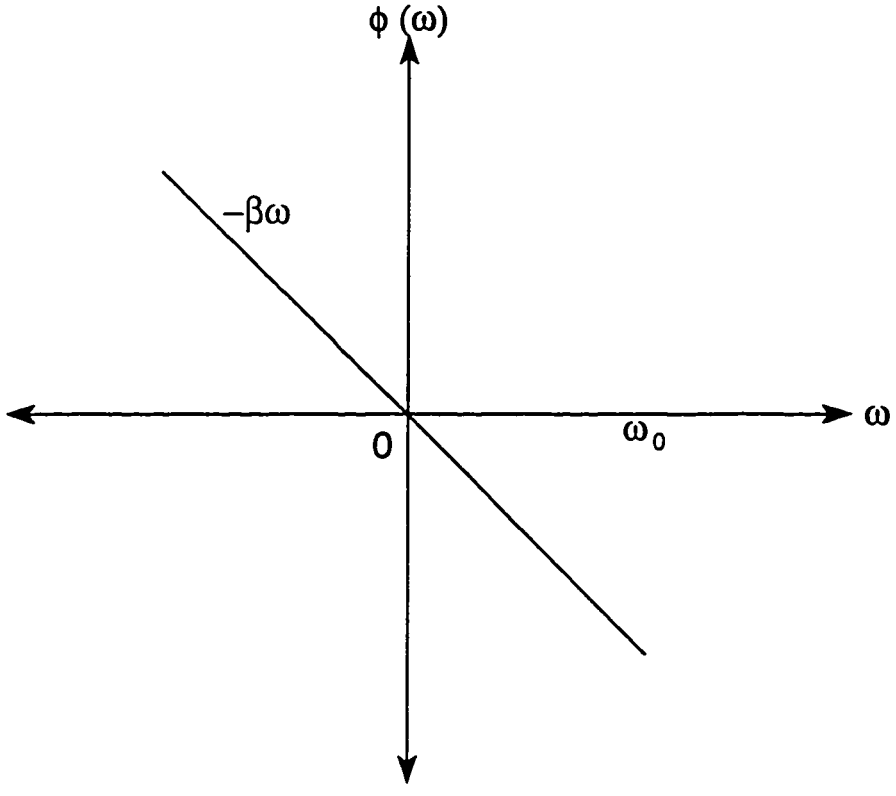

Figure 1.6: Ideal Phase Characteristics [4]

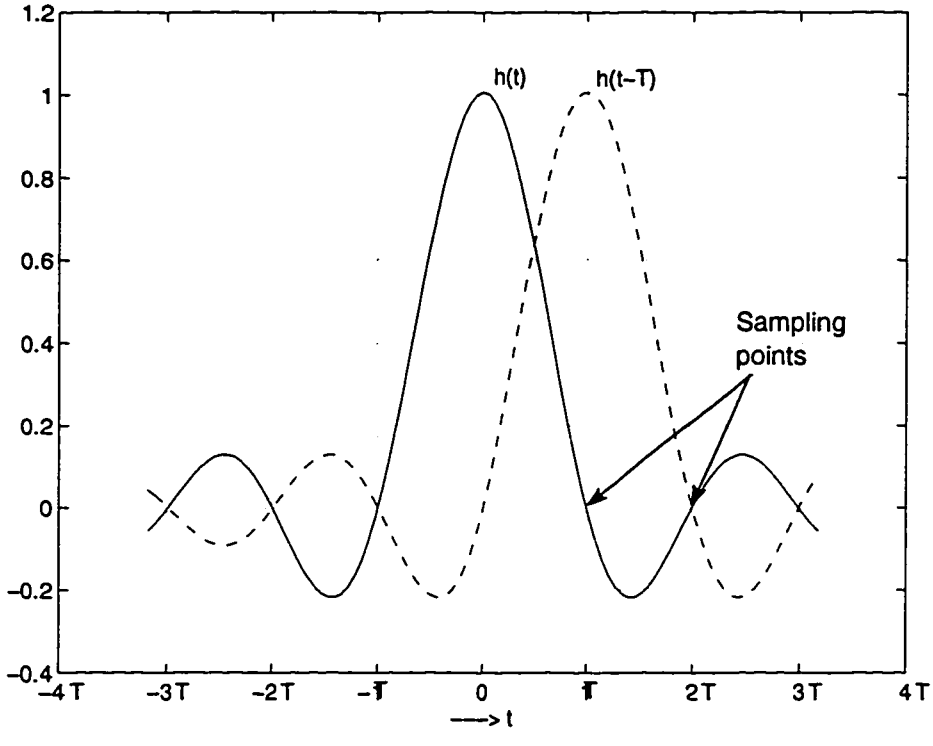

Figure 1.7: Time shifted Versions of Impulse Response [7]

A filter response with ideal cutoff frequency characteristics has a rectangular shape and produces a *Sinc* function in the time domain. However, the Sinc function is physically not realizable as it is extends from minus infinity to plus infinity and hence is a noncausal function. Therefore, filters with non ideal response are used which give a more shorter time domain pulse response and are spread in the frequency domain [16]. We see that a compromise is done with the increase in bandwidth of the filter to get shorter time domain responses. The pulse is then delayed in the time domain to make it causal. Again care has to be taken so that the pulse shape should have zero crossings at the sampling intervals. In order to achieve this condition Nyquist stated if the filter is band limited to less than two Nyquist bandwidths and has linear phase characteristics, then its amplitude response should have vestigial symmetry about the Nyquist frequency w_0 [2].

However, the Nyquist criteria does not provide a unique design for the pulse shape of signals with bandwidth greater than half the signaling rate which is the minimum signal bandwidth [2]. The phase response of the filter is also important since the deviation from the ideal linear phase causes unpredictable distortion of the pulse shape. Further, such a deviation is incompatible with the minimum ISI requirement [1].

Unfortunately, any ideal filter behavior is physically unrealizable. This is because, as we shall see, the practical filter network functions $H(s)$ are ratios of polynomials of limited order. Hence the filter designer must obtain a response which is

practical and which approximates the ideal filter characteristics within some specified set of tolerances.

1.3 Jitter

In ideal data transmission systems, the pulses of the digital pulse stream would arrive at times that are integer multiples of the pulse repetition period T. However in real systems, the pulses arrive at times that differ from the integer multiples of T. As a result of the signals being displayed from their optimum position in time, errors are introduced in the system. This unwanted pulse position modulation of the pulse stream is called jitter [3] and can be seen in figure 1.8.

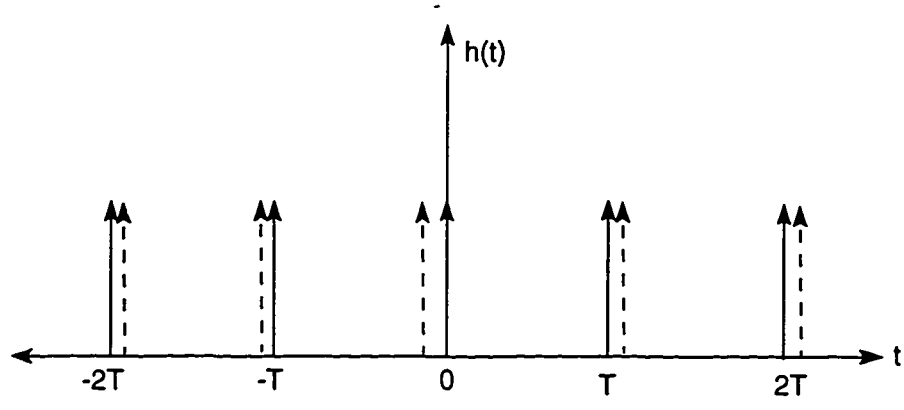

Figure 1.8: Shifting of pulse due to jitter effect [3]

The primary sources of jitter in digital transmission system are regenerators and multiplexers [3]. Jitter effects are more evident with improper synchronization and timing errors at the receiver. This jitter amounts to considerable intersymbol

interference at the sampling points and may degrade transmission performance [3].

Jitter effects can be minimized by designing the transmission pulse shapes such that its side lobes are much smaller when compared to the maximum pulse amplitude. This is obtained by making the signal decay rapidly beyond the main lobe.

1.4 Evaluation Parameters

A data transmission filter can be evaluated and compared based on a set of filter characteristics known as evaluation parameters. In this section, we define some of the evaluation parameters which will be used later to compare the merits of different transmission filters. These definitions follow the formulation in reference [1].

1. Minimum Attenuation: This is the maximum filter gain outside the specified bandwidth, measured in decibels (dB).

2. Maximum Overshoot: This is the filter gain overshoot over $H(0)$ in the band $0 \leq w \leq 2w_0$, measured in dB.

3. Side Lobe %: This is the percentage ratio of the maximum amplitude of the filter impulse response $h(t)$ for $|t| > (T \pm k.\beta)$ (where k is an integer) to the maximum value of $h(\beta)$, β being the time delay of the impulse response.

4. Sampling Error: It is defined as

$$\frac{\sum_{k=-|k_m|}^{\infty} h^2(\beta + kT)}{h^2(\beta)} \tag{1.4}$$

where k_m is the largest integer less than $\frac{\beta}{T}$ and k is not equal to zero.

5. Maximum Phase deviation: It is defined as the maximum difference between the angle of the filter transfer function and the linear phase value βw within the band of 0 to $2w_0$.

Chapter 2 will provide a detailed study of data transmission filters. The design procedures adopted by various researchers will be presented.

Chapter 2

Filters: Overview

In this chapter, the concepts of general filter design, its types and characteristics are discussed. Furthermore, the literature survey of the various available techniques used to design pulse shapes in data transmission filters along with their results is presented. The two main important characteristics of a filter are those of amplitude and phase. We first deal with the problem of amplitude approximation in section 2.1 followed by the phase approximation problem in section 2.2. The combined magnitude and phase approximations for Nyquist filters are studied in section 2.3.

2.1 Amplitude Oriented Design

The three well known amplitude approximations are that of Butterworth filter, Chebychev filter and Elliptic filter. The Butterworth filter has a maximally flat

amplitude response in both the passband and the stop band. A considerable improvement in the rate of cutoff, over the maximally flat pass band response results if we require $|H(j\omega)|$ to be equiripple in the pass band while retaining the maximally flat response in the stop band. Such class of filters are called Checbychev filters. The Elliptical response gives rise to equiripple responses in both the pass band and the stop band. The details of the design and approximation procedure for these filters are well documented and may be found in reference [4].

2.2 Phase Oriented Design

To obtain the approximation to the ideal linear phase characteristic shown in figure 1.6, we consider the functions to be of the form

$$H(s) = \frac{1}{Q_n(s)} \tag{2.1}$$

The phase $\phi(w)$ of the function $H(s)$ is required to be linear in the pass band, alternatively the group delay $T_g(s)$ should approximate to a constant in the pass band, where

$$T_g(s) = -\frac{d\phi(s)}{ds} \tag{2.2}$$

There are several ways for the derivation of the n^{th} degree polynomial of the above form which results in a linear phase or constant group delay response. However the

two most widely used methods are that of maximally flat group-delay response and the equidistant linear phase response [4].

2.2.1 Maximally flat group delay approximation

The polynomial $Q_n(s)$ which gives rise to a group-delay function with maximum number of zero derivatives at $w = 0$ can be generated by the recurrence relationship [4], [5]

$$Q_{n+1}(s) = Q_n(s) + \frac{s}{4n^2 - 1} 2Q_{n-1}(s) \tag{2.3}$$

with

$$Q_0(s) = 1 \text{ and } Q_1(s) = 1 + s \tag{2.4}$$

The above polynomial $Q(s)$ is strictly Hurwitz, thereby guarantying stability of the filter. The polynomial $Q(s)$ is also related to the well known Bessel Polynomial $B(s)$ by the relation [4]

$$Q(s) = s^n . B_n(1/s) \tag{2.5}$$

and hence the realized network is sometimes called a Bessel filter.

2.2.2 Equidistant linear phase approximation

The phase of the equidistant linear phase polynomial interpolates the ideal linear phase response $\phi(w) = -w$ over a finite band about $s = 0$. This is obtained by deriving the polynomial $A_n(jw)$ such that [4], [5]

$$\phi(w) - Arg\{A_n(\alpha_0 \mid jw_i)\} = 0 \tag{2.6}$$

at specific w_i where $w_i = i\alpha_0$, and $i = 0, 1, 2, ..., n$. The phase is exactly linear at these set of equidistant points in the pass band region and α_0 is the spacing between the interpolation points [5]. $A_n(s)$ is called the *equidistant linear phase polynomial*, and can be generated by means of the recurrence formula [4] [5],

$$A_{n+1}(\alpha_0 \mid s) = A_n(\alpha_0 \mid s) + \frac{\tan^2(\alpha_0)}{\alpha_0^2} \cdot \frac{s^2 + (\alpha_0 n)^2}{(4n^2 - 1)} A_{n-1}(\alpha_0 \mid s) \tag{2.7}$$

with

$$A_0(\alpha_0 \mid s) = 1, \tag{2.8}$$

and

$$A_1(\alpha_0 \mid s) = 1 + \frac{\tan \alpha_0}{\alpha_0} s \tag{2.9}$$

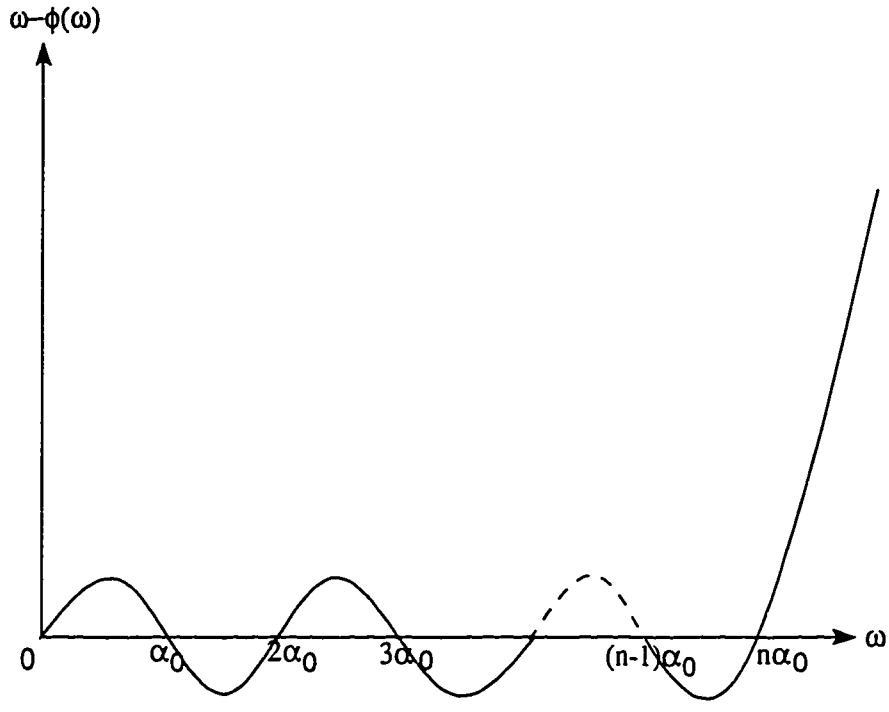

Figure 2.1: Phase error in equidistant linear phase approximation [4]

The necessary and sufficient condition for $A_n(s \mid \alpha_0)$ to be strictly Hurwitz is [5]

$$\alpha_0 < \frac{\pi}{2} \tag{2.10}$$

We see that if $\alpha_0 \rightarrow 0$ in equation (2.7), the maximally flat solution is recovered as given in equation (2.3). Typical behavior of the phase error of this polynomial is shown in figure (2.1).

2.2.3 Modified Equidistant Linear Phase Response

Baher has modified the equidistant linear phase approximation [1] by identifying

$$\alpha_0 = \alpha.\beta \tag{2.11}$$

so that α_0 is written as the product of two parameters. Thus

$$Q_n(\alpha \mid \beta \mid s) = A_n(\alpha\beta \mid \beta s) \tag{2.12}$$

where α is the spacing between the interpolation points and β is the slope of the phase of the system. The necessary and sufficient condition for stability of the filter becomes [1]

$$\alpha.\beta < \frac{\pi}{2} \tag{2.13}$$

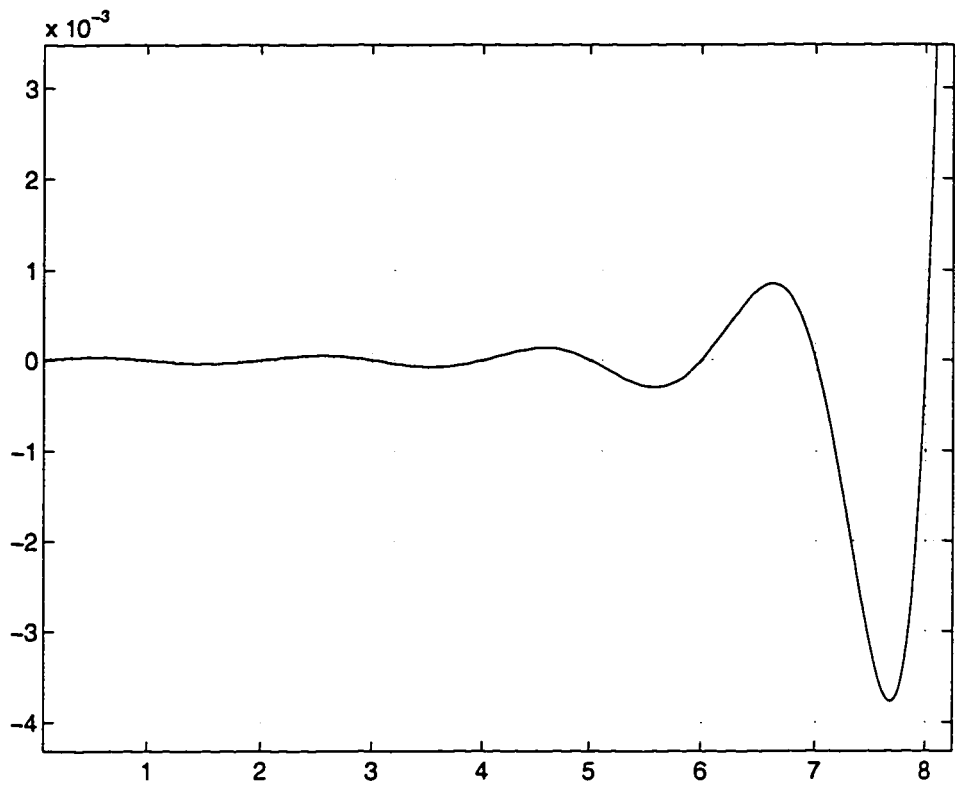

Figure 2.2: Equidistant linear phase error for n=8, α=1 and β=1 [1]

and $Q_n(\alpha \mid \beta \mid s)$ interpolates the function βw at $n+1$ equidistant points, i.e.,

$$\beta w_i - Arg\{Q_n(\alpha_0 \mid s)\} = 0 \quad w_i = i\alpha \quad i = 0, 1, 2, ..., n \tag{2.14}$$

Figure (2.2) shows the phase error of this function with α=1 and $\beta = 1$ for an 8^{th} order polynomial.

2.3 Nyquist Filters

The frequency characteristics of a filter having exactly zero ISI (intersymbol interference) were first introduced by Nyquist in 1928 [6] and this theory was later extended to general class of filters by Gibby and Smith in 1965 [2].

2.3.1 Nyquist's Theory

Nyquist established that the theoretical minimum system bandwidth needed to detect $1/T$ pulses (symbols) per second without intersymbol interference is $1/2T$ hertz [2]. In other words, a system with bandwidth $W = 1/2T$ can support a maximum transmission rate of $2W = 1/T$ symbols/sec. This is known as the Nyquist bandwidth constraint and $w_0 = 1/2T$ is called the Nyquist bandwidth. A filter with ideal cutoff frequency characteristics, satisfying the minimum Nyquist bandwidth constraint, has a rectangular shape and produces a $Sinc$ function in the time domain. However, this $Sinc(t/T)$ function is physically unrealizable as it is extends from

minus infinity to plus infinity and hence would require an infinite time delay to make it causal [17]. Also, with such a characteristic, the detection process would be very sensitive to the effect of jitter or timing errors in practical receiver systems. The pulse is then shifted in the time domain to make it causal. Again care has to be taken so that the pulse shape should have zero crossings at the sampling intervals [2].

This condition was also specified by Nyquist as follows: If the filter is band limited to less than two Nyquist bandwidths and has linear phase characteristics, then its amplitude response should have vestigial symmetry about the Nyquist frequency w_0 [7].

Nyquist's classic paper considered the conditions necessary for digital data transmission without intersymbol distortion and these conditions have provided the guide for system design for many years. However, the Nyquist criteria does not provide a unique design for the pulse shape for signals with bandwidth greater than half the signaling rate or the minimum Nyquist bandwidth [2]. Also, he has treated the case in which no energy is transmitted at a frequency above twice the signalling speed, although he mentioned the general case in passing. As a consequence, his results cannot be applied directly to cases in which the amplitude characteristics extend beyond twice the signalling speed (gradual cutoff systems) or baseband systems without low frequency components. In addition, Nyquist's theory has been incompletely exploited in practice. The usual application of the principles of chan-

nel shaping amounts to equalizing the amplitude to produce a symmetric roll-off characteristic. This procedure is valid and consistent with the theory, but is only a special application of the theory [2].

Later in 1965, the work by Gibby and Smith [2] gave some extensions to the Nyquist's Telegraph Transmission theory . They extended the previous results by showing that it is not necessary to restrict the bandwidth to arrive at an efficient description of the amplitude and phase constraints for distortionless transmission. In other words, transmission systems without a sharp cutoff frequency were considered and constraints on the system characteristics were obtained [2].

In practical systems where the bandwidth available for transmitting data at a rate of $1/T$ bits/sec is between $1/2T$ to $1/T$ Hz, a class of $H(jw)$ with a raised cosine characteristics is mostly used. A raised cosine frequency spectrum consists of a flat amplitude portion and a roll-off portion that has a sinusoidal form. Then pulse spectrum $H(jw)$ is specified in terms of the rolloff parameter γ as [8]

$$\begin{aligned} H(jw) &= T && 0 \leq |w| \leq (1-\gamma)\pi/T \qquad (2.15) \\ &= \frac{T}{2}\left[1 - Sin\ \frac{T}{2}\left(w - \frac{\pi}{T}\right)/\gamma\right] && (1-\gamma)\pi/T \leq |w| \leq (1+\gamma)\pi/T \\ &= 0 && |w| \geq (1+\gamma)\pi/T \end{aligned}$$

where $0 < \gamma < 1/2T$. The pulse shape $h(t)$ corresponding to the $H(jw)$ given

above is [8]

$$h(t) = \frac{Sin\ \pi t/T}{\pi t/T} \frac{Cos\ \gamma \pi t/T}{1 - 4\gamma^2 t^2/T^2} \tag{2.16}$$

Figure (2.3) and figure (2.4) show the different raised cosine frequency responses and their time domain responses for different roll off factors γ.

These requirements cannot be exactly met by finite-degree rational functions but can be used to find target functions in either time domain (example: $[Sin(t)]/t$) or frequency domain (for example, raised cosine). The design methods have produced useful results but suffers from two main defects. Firstly, there are infinite number of target functions available and the second being the large number of approximation procedures. These methods may give small ISI but not necessarily the minimal [9].

Various other researchers have adopted different approaches to solve this problem. A solution in time domain or in frequency domain or simultaneously in both time domain and frequency domain have been attempted. Ulstad, Nader, Lind and Hassan have tried to formulate the problem in time domain [9] [7] [10]. The idea of energy maximization in the time domain to generate various pulse shapes was studied. The second approach has been to approximate a frequency domain unrealizable shape such as the raised-cosine pulse so that the time domain response approaches the required property of regular zero crossings [11]. However, it is possible to give examples of other unrealizable target functions which have superior

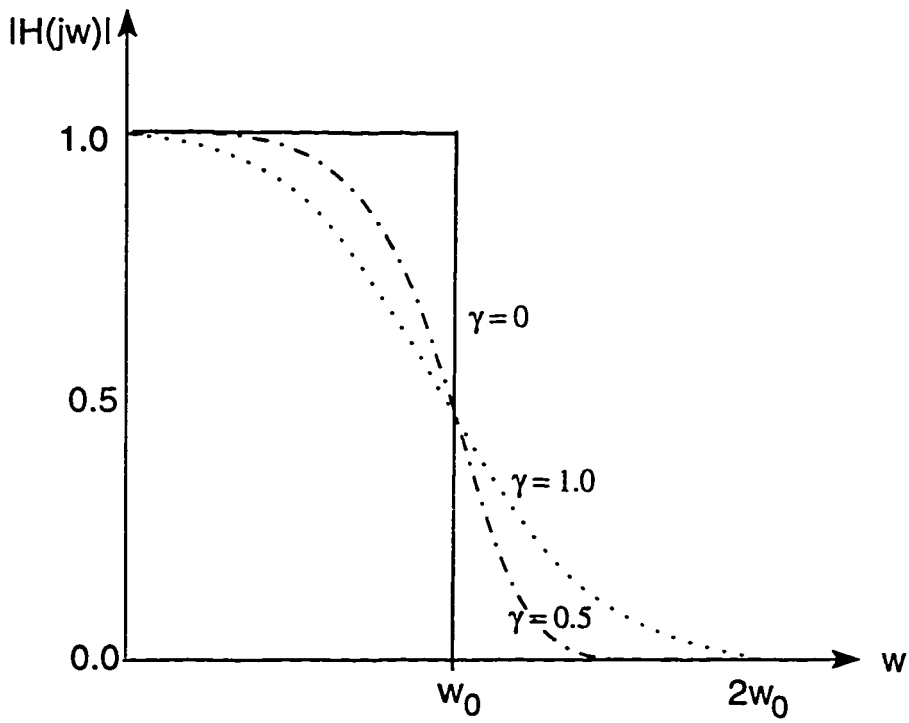

Figure 2.3: Normalized Frequency responses for different rolloff factors γ [17]

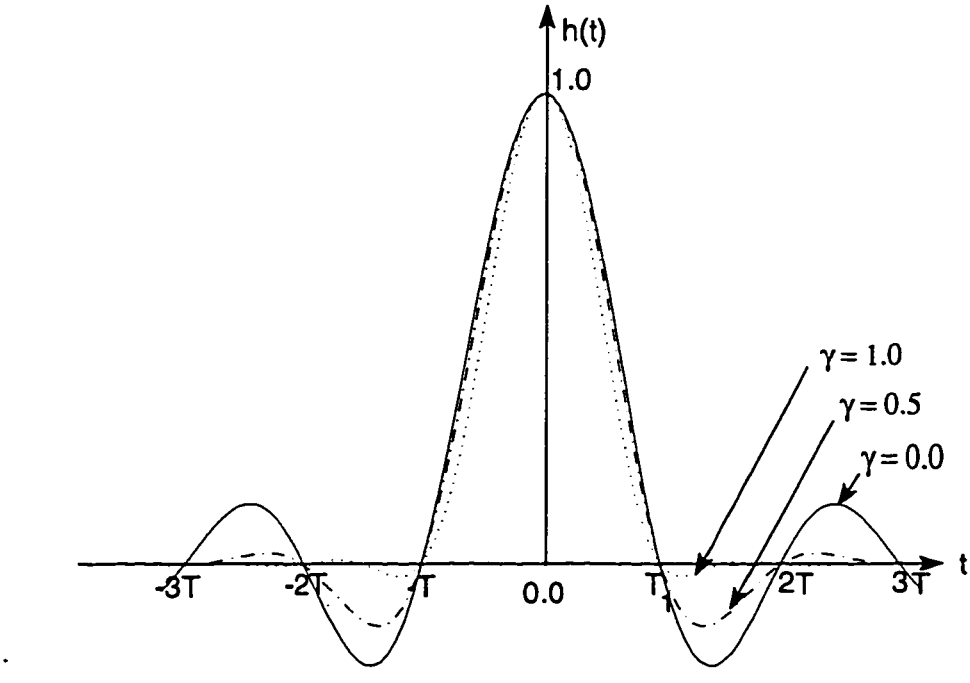

Figure 2.4: Time responses for different rolloff factors γ [17]

aspects of their time response by comparison with the ideal raised cosine [12]. The third approach imposes both the time domain requirements and some aspects of the frequency response (such as the stop band shape) simultaneously [13]. Again this leads to a nonlinear set of equations, and imposing the specifications require an iterative procedure [1].

2.3.2 Time domain solutions

In many aspects it is best to solve the approximation problem directly in the time domain without using the infinite number of available target functions. Ulstad [9], Spauling [13], Hassan [10], Nader and Lind [7] were the researchers who followed this approach.

Ulstad [9] produced rational polynomial Laplace transform approximations for truncated versions of $sin(kt+b)/(kt+b)$, by using nonlinear programming techniques designed to avoid the usual false minimum problems. The wave form $sin(kt+b)/(kt+b)$ is truncated, delayed, and scaled so that the peak response occurs at $t = 1$, is zero before $t = 0$, and is multiplied by a delaying exponential after $t = 2$. Use of decaying exponential is made in the interest of producing smaller approximation error in the range $0 \leq t \leq 2$ at the possible expense of a small amount of phase non-linearity. The approximation technique and the resulting functions were used to construct an active network realization of time response using biquadratic transfer function building blocks. The filter characteristics obtained are shown in figures (2.5-2.6).

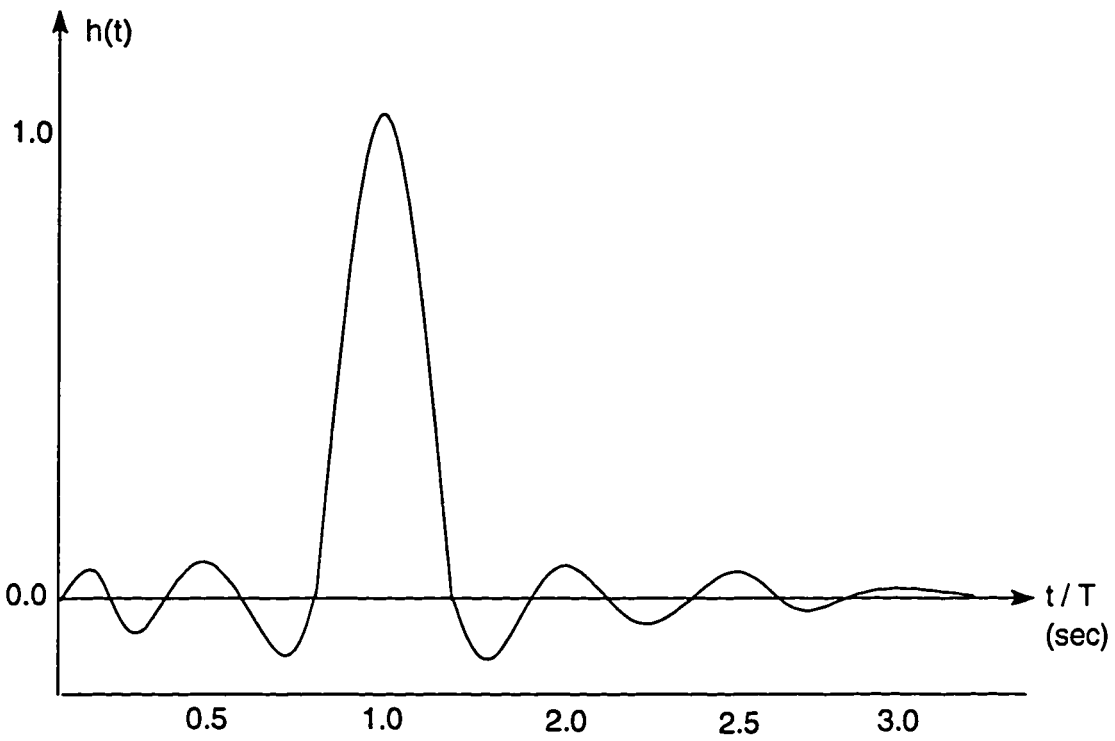

Figure 2.5: Function derived from $sin(5\pi t - 5\pi)/(5\pi t - 5\pi)$ [9]

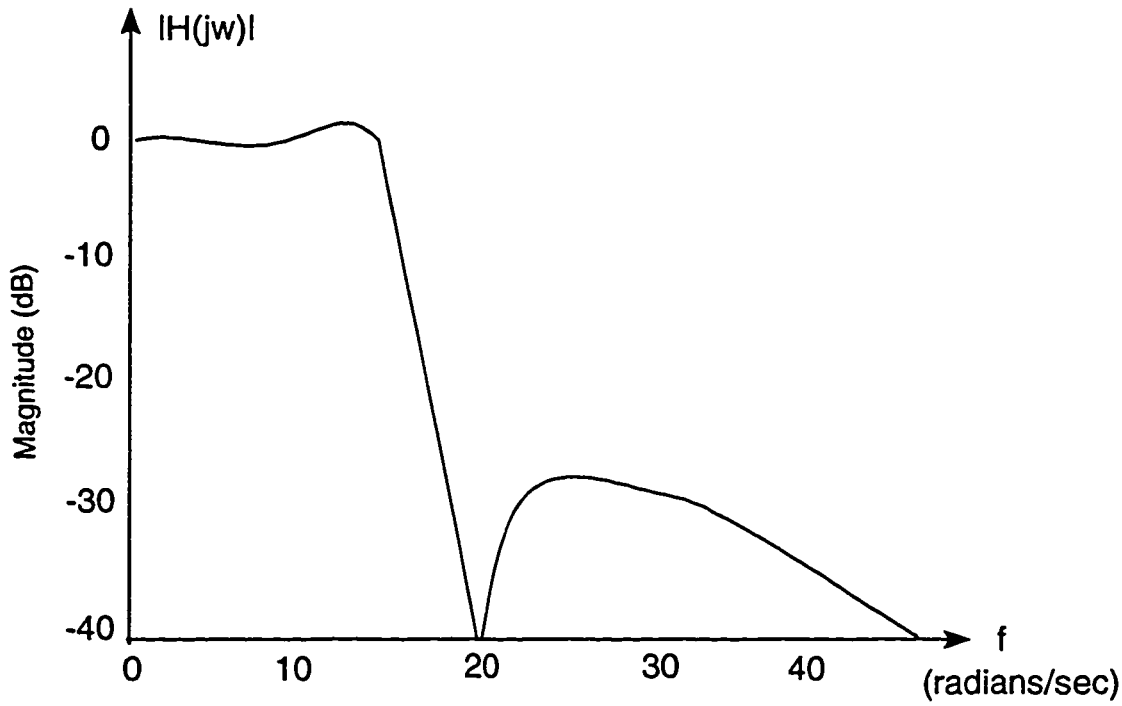

Figure 2.6: Magnitude of Fourier transform of function shown in Fig 2.5 [9]

Nader and Lind [7] have designed an impulse response such that it produces a relatively large response at $t = t_M$ and near zero responses at $t = t_M + kT$ (k is any integer). The intersymbol interference was minimized over an infinite point set consisting of the precursor and postcursor sample points. This design was implemented using an iterative computer program, keeping $t_M = 1$ and increasing n, the degree of the filter. The results showed that in the frequency domain both the amplitude and group delay response acquired an increasingly large peak near band edge, and in the time domain the ringing amplitude of the impulse response increased [7]. The resulting filter does not require a separate group delay equalizer. A key feature in the design is the placement of the main sample point to lie at the peak of the filter. The optimal design for impulsive inputs was then extended to other general inputs like that of the pulse. However when n was increased above seven, the computer program did not converge for many designs that were attempted [7].

A very useful contribution in the field of designing band-limited Nyquist signal shapes for data transmission was made by Spauling [13]. The design of networks to shape an arbitrary input pulse into a band-limiting pulse having minimum intersymbol interference was proposed. The zeros of the network transfer function were used to achieve the band-limiting properties while the transfer function poles are optimized with a computer to give the desired time response. The resulting functions were used to construct an active network realization [13].

Tugbay and Panayiri [14] designed signal shapes by optimizing the energy in a given time interval for fixed excess bandwidth factor γ and also incorporating the Nyquist criteria so that no intersymbol interference occurs at the periodic sampling points. The optimal signal is a solution of an inhomogeneous linear integral equations of Fredholm type. The computation involved the determination of eigenvalues and eigenfunctions of a positive definite and symmetric kernel in terms of prolate spheroidal wave functions. The optimal signal $s(t)$ was selected by maximizing the function

$$J = E_i - \lambda.E_0 \tag{2.17}$$

where E_i is the energy in the time interval $(-\sigma T, \sigma T)$, E_0 is the total energy and λ is a lagrange multiplier that corresponds to the fraction of the energy in $s(t)$ which falls in the interval $|t| \leq \sigma T$ i.e, $\lambda = (E_i/E_0)_{s(t)}$. Therefore λ is a positive and less than one. E_i and E_0 are expressed as

$$E_i = \int_{-\sigma T}^{+\sigma T} s^2(t)dt \tag{2.18}$$

and

$$E_0 = \int_{-\infty}^{+\infty} s^2(t)dt \tag{2.19}$$

Solving equation (2.17) for largest root of λ, we get λ_{max} which corresponds to the optimal solution i.e., $s(t)|_{\lambda=\lambda_{max}}$ has the maximum energy in the interval

$(-\sigma T, \sigma T)$. Figure (2.7-2.8) show the optimal signal shapes produced in reference [14] with $\sigma = 1$ and the raised cosine having a roll off factor $\gamma = 0.75$.

Later, Hassan [10] suggested a much simpler technique for energy maximization of the Nyquist pulse shape requiring little numerical effort. The problem was formulated in terms of a set of amplitude coefficients $a_i's$ in the frequency domain whose inverse Fourier transform is used get the time domain function. The time domain energy $E(\sigma T)$ within a particular interval $(-\sigma T, \sigma T)$ and the total energy under the full bandwidth $E(\infty)$ are related by

$$\frac{E(\sigma T)}{E(\infty)} = \lambda = \frac{\alpha^T R \alpha}{\alpha^T \alpha} \tag{2.20}$$

or

$$\lambda \alpha^T \alpha = \alpha^T R \alpha \tag{2.21}$$

where R will be known matrix and α is the transpose vector of the amplitude coefficients. The maximization of energy in any particular band of interest $-\sigma T$ to σT is found by finding the maximum eigenvalue of R, denoted by λ_{max}. In this case, α is the eigenvector corresponding to λ_{max}. Solving for α gives the coefficients $a_i's$ which produces frequency response of the Nyquist pulse shape. The time domain pulse shape is readily obtained using the inverse Fourier transform, which completes the solution.

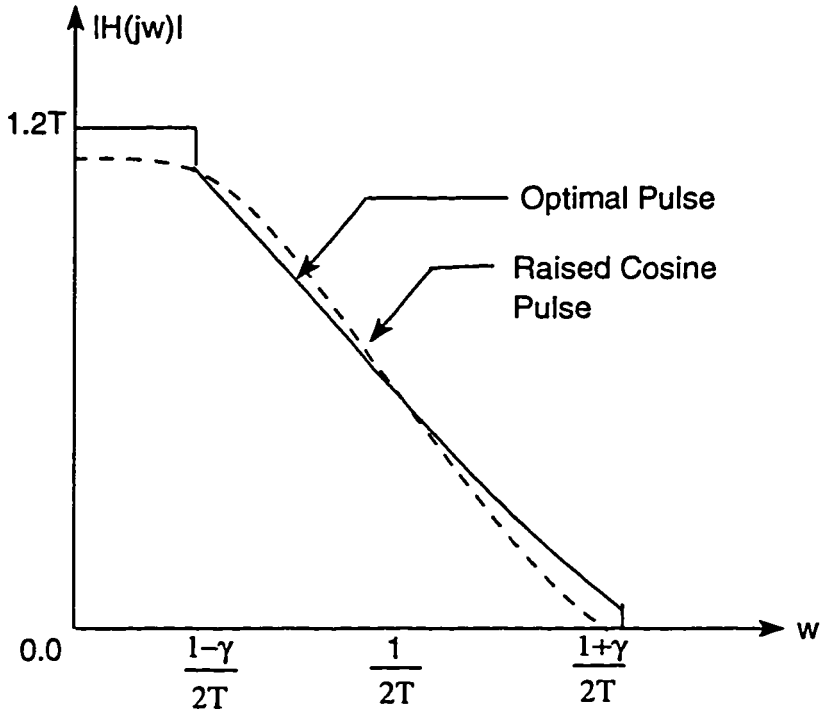

Figure 2.7: Tugbay's signal shape in frequency domain [14]

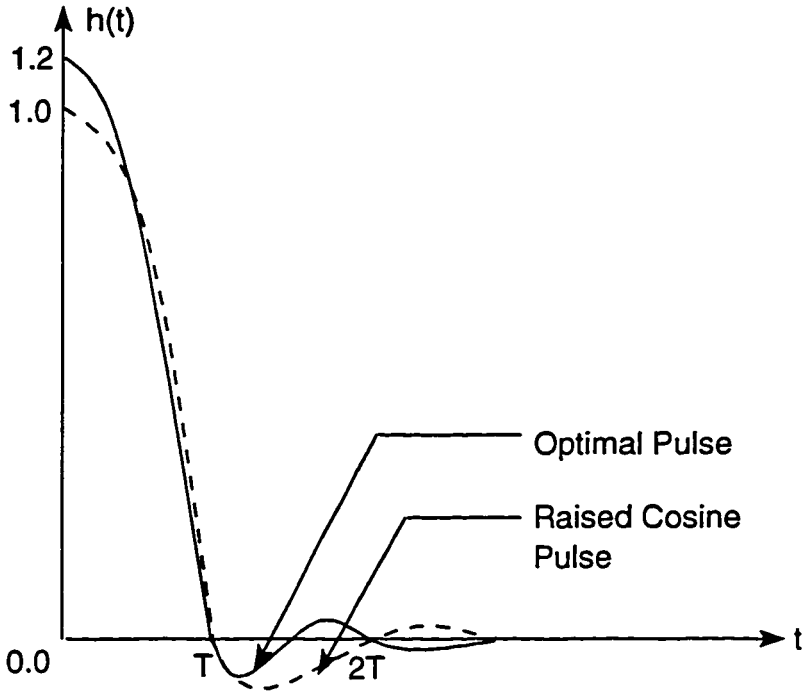

Figure 2.8: Tugbay's signal shape in time domain [14]

The above solutions of [14] and [10] give target frequency domain shapes for rapidly decaying impulse responses but do not solve for filter realizable functions.

2.3.3 Frequency domain solutions

In frequency domain solutions, a possible approach is to design the filter on amplitude basis and subsequently phase-equalizing the resulting network. This is achieved by cascading it with an all-pass section. The phase response of the all-pass phase equalizer is determined such that it compensates for the deviation from phase linearity of the amplitude oriented design. Alternatively linear phase networks can be amplitude equalized. However, in both approaches the solution is far from optimum, i.e. the degree of the network is higher than one would anticipate by examining the available degrees of freedom [4]. For this reason, only solutions to the problem of simultaneous amplitude and phase approximations are pointed here.

The approach in reference [1] gave an excellent solution to the problem of filter design by forcing the phase of the filter to linearity and optimizing the transfer function magnitude. The filter transfer function is derived entirely in the frequency domain in such a way that the ISI, amplitude selectivity and phase characteristics are met simultaneously without the need for subsequent equalization or correction of either the amplitude or delay.

The technique assumes the denominator of the filter transfer function to be known polynomial, while the numerator of the filter transfer function is determined

by solving a set of linear algebraic equations.

The filter transfer function is selected as

$$H(s) = \frac{P_{2m}(s)}{Q_n(s)} \qquad 2m < n \tag{2.22}$$

with

$$P_{2m}(s) = \sum_{0}^{m} b_r s^{2r}$$

where s=$(\sigma + jw)$ is the usual complex frequency. $P_{2m}(s)$ is an even polynomial for a reciprocal realization of $H(s)$ and $Q_n(s)$ is the equidistant linear phase polynomial of degree n as defined in section (2.2.3).

Using the functions

$$\gamma_1(w) = \cos(\beta(w_0 - w)) \tag{2.23}$$

$$\gamma_2(w) = \cos(\beta(w_0 + w)) \tag{2.24}$$

$$F_1(w) = Re\{H(j(w_0 - w))\} \tag{2.25}$$

$$F_2(w) = Re\{H(j(w_0 + w))\} \tag{2.26}$$

where w_0 is the Nyquist frequency and β is the delay of the filter based on equation (2.13). It was proved that if

$$F_2(w).\gamma_1(w) + F_1(w).\gamma_2(w) \approx \gamma_1(w).\gamma_2(w) \qquad 0 < |w| < w_1 \tag{2.27}$$

then, the impulse response $h(t)$ of the filter is such that

$$h_\beta(kT) \approx 0 \qquad k = \pm 1, \pm 2, \pm 3, ... \tag{2.28}$$

where

$$h_\beta(t) = h(t + \beta) \tag{2.29}$$

$h_\beta(kT)$ deviates from zero by an error that can be made arbitrarily small by taking n and m in equation (2.22) sufficiently large. The condition of equation (2.27) along with the constraint on slope at w_0 was applied to the transfer function of equation (2.22). The results of this work are tabulated in table (2.1).

order n	8	10	12	14
k_m-β	1.6-0.8	2-1	2.1-1.2	2.8-1.4
Slope at w_0	-0.25	-0.25	-0.25	-0.25
Min. attenuation in dB	21.76	25.82	28.66	36.87
Max. overshoot in dB	0.359	0.399	0.316	0.128
Side Lobe in %	24.47	15.26	14.22	13.06
Sampling Error	1.2 E-3	4.0 E-4	3.0 E-6	2.8 E-7
Max. Phase Deviation	6.3 E-2	4.2 E-2	3.2 E-2	2.4 E-2

Table 2.1: Results from reference [1]

Later, Hassan [11] made an attempt to reduce the phase deviation of the linear phase polynomial by modifying the numerator of the transfer function as

$$H(s) = \frac{\sum_{i=0}^{m} a_{2i}.s^{2i} + \sum_{i=0}^{m} b_{2i+1}.s^{2i+1}}{Q_n(s)} \tag{2.30}$$

and approximating it to fixed target shapes such as the raised cosine curves. However the transfer functions of the form of equation (2.30) require almost double the number of components as compared to equation (2.22) for the reciprocal realization. The technique is based on choosing the magnitude target function as raised cosine and the phase to be strictly linear. The denominator of the equation (2.30) is the linear phase polynomial. The numerator coefficients $a_i's$ and $b_i's$ are determined using least mean square method such that the modelled filter approximates the target functions. The results obtained for target functions of modified raised cosine with excess bandwidth $\gamma = 1$ are shown in table (2.2).

order n	8	10	12	14
α, β	1.57, 0.8	1.25, 1	1.047,1.2	0.89, 1.4
Slope at w_0	-0.128	-0.123	-0.126	-0.128
Min. attenuation in dB	40.1	25.82	28.66	36.87
Max. overshoot in dB	0.0	0.0	0.0	0.0
Side Lobe in %	3.16	2.7	2.84	2.7
Sampling Error	4.5 E-5	2.48 E-5	1.9 E-5	3.8 E-6
Max. Phase Deviation	3.7 E-2	2.0 E-2	1.3 E-2	6.4 E-3

Table 2.2: Results of reference [11]

2.4 Synthesis of Filters

The procedure of realizing the transfer function $H(s)$ as a doubly-terminated lossless two-port starts with finding the input impedance of the resistor-terminated two-port [4].

2.4.1 Derivation of the Input Impedance

Let the designed filter transfer function be represented in the form

$$H(s) = \frac{P(s)}{Q(s)} \tag{2.31}$$

and hence the transducer power gain is

$$|H(jw)|^2 = \frac{|P(jw)|^2}{|Q(jw)|^2} \tag{2.32}$$

The input reflection coefficient $S_{11}(s)$ can be found out from the relation [4],

$$|S_{11}(jw)|^2 = 1 - |H(jw)|^2 \tag{2.33}$$

so that

$$S_{11}(s)S_{11}(-s) = 1 - H(s)H(-s)$$

$$\begin{aligned} &= 1 - \frac{P(s)P(-s)}{Q(s)Q(-s)} \\ &= \frac{Q(s)Q(-s) - P(s)P(-s)}{Q(s)Q(-s)} \end{aligned} \tag{2.34}$$

The poles of $S_{11}(s)$ are restricted to lie in the open left hand plane. Therefore, these are the zeros of $Q(s)$ which are the same poles of $H(jw)$, so that

$$S_{11}(s) = \frac{U(s)}{Q(s)} \tag{2.35}$$

where $U(s)$ is obtained by the factorization of equation (2.34) and assigning half of the zeros to U(s). In doing so, we are free to take any combination of half the zeros of the numerator of equation (2.34), provided that the corresponding factors combine to form a real polynomial. Therefore this factorization is not unique, and may result in different networks having the same response. The input impedance $Z(s)$ is obtained from $S_{11}(s)$ by using the relation [4]

$$\begin{aligned} Z(s) &= \frac{1 + S_{11}(s)}{1 - S_{11}(s)} \\ &= \frac{Q(s) + U(s)}{Q(s) - U(s)} \end{aligned} \tag{2.36}$$

The obtained input impedance $Z(s)$ is the starting point of the synthesis of the passive network to be obtained.

2.4.2 Synthesis

The process of network synthesis is to extract by parts a physical network from the given driving point impedance $Z(s)$. Then the remaining impedance is evaluated and the extraction procedure is repeated until the complete function is exhausted [4].

The Brune Preamble

The primary synthesis procedure begins by first extracting all the jw axis poles of $Z(s)$ including those at origin and infinity through the Cauer's canonical form. The driving point impedance $Z(s)$, obtained in the previous section may be expressed as

$$Z(s) = \frac{a_n s^n + a_{n-1} s^{n-1} + ... + a_0}{b_m s^m + b_{m-1} s^{m-1} + ... + b_0} \tag{2.37}$$

and

$$Y(s) = \frac{1}{Z(s)} \tag{2.38}$$

where $Y(s)$ is the admittance.

To produce a network, we start from $Z(s)$ or $Y(s)$ depending upon which has a pole at $s = \infty$. For $Z(s)$ or $Y(s)$ to have a pole at $s = \infty$, m and n differ by one. If $Z(s)$ has a pole at $s = \infty$, then $n = m + 1$ and the first element shown in fig(2.9) is an inductor. If $Y(s)$ has a pole at pole at $s = \infty$, then $n = m - 1$. Assuming that $Z(s)$ satisfies this requirement, then we divide the numerator by the denominator

of $Z(s)$ as

$$Z(s) = k_1 s + Z_1(s) \tag{2.39}$$

where $Z_1(s)$ is the remainder impedance, which is identified as the impedance of the network minus the first series inductor. The value of the inductor is given by $L_1 = k_1$. The admittance $Y_1(s) = 1/Z_1(s)$ now has a pole at $s = \infty$. Thus we can write

$$Z(s) = k_1 s + \frac{1}{Y_1(s)} \tag{2.40}$$

and we repeat the same process of dividing the numerator of $Y_1(s)$ by it denominator to obtain

$$Z(s) = k_1 s + \frac{1}{k_2 s + Y_2(s)} \tag{2.41}$$

where $k2$ is the value of the shunt capacitor shown in figure (2.9). The process of division and iteration is repeated until we obtain a minimum reactance and minimum susceptance function Z_m as

$$Z(s) = k_1 s + \cfrac{1}{k_2 s + \cfrac{1}{k_3 s + \ddots \cfrac{1}{k_{i-1} s + Z_m}}} \tag{2.42}$$

A minimum reactance function is the impedance devoid of jw-axis poles (including zero and ∞) and a minimum susceptance is the admittance devoid of jw-axis poles (including zero and ∞). The synthesis procedure until here is called as the Brune preamble.The realization of the minimum reactance and minimum suscep-

tance (MRMS) functions are covered in the next section.

MRMS Functions

The minimum-reactance and minimum susceptance (MRMS) function $Z_m(s)$ which remain after the Brune preamble is represented as

$$Z_m(s) = \frac{m_1 + n_1}{m_2 + n_2} \tag{2.43}$$

where m_1 and m_2 are even polynomials in s and n_1 and n_2 are odd polynomials in s. $Z_m(s)$ is to be realized as a resistively terminated losssless network. The lossless two port network is obtained as a cascade of lossless reciprocal subnetworks. Each one of the constituent two-port realizes a particular zero of transmission (i.e a zero of $Ev\, Z_m(s)$). The zeros of transmission are the zeros of [4]

$$Z_m(s) + Z_m(-s) \tag{2.44}$$

or of

$$m_1 m_2 - n_1 n_2 \tag{2.45}$$

These zeros are assumed to be of even multiplicity, for a reciprocal realization. If a particular zero of transmission s_0 is to be extracted from $Z_m(s)$ by a section

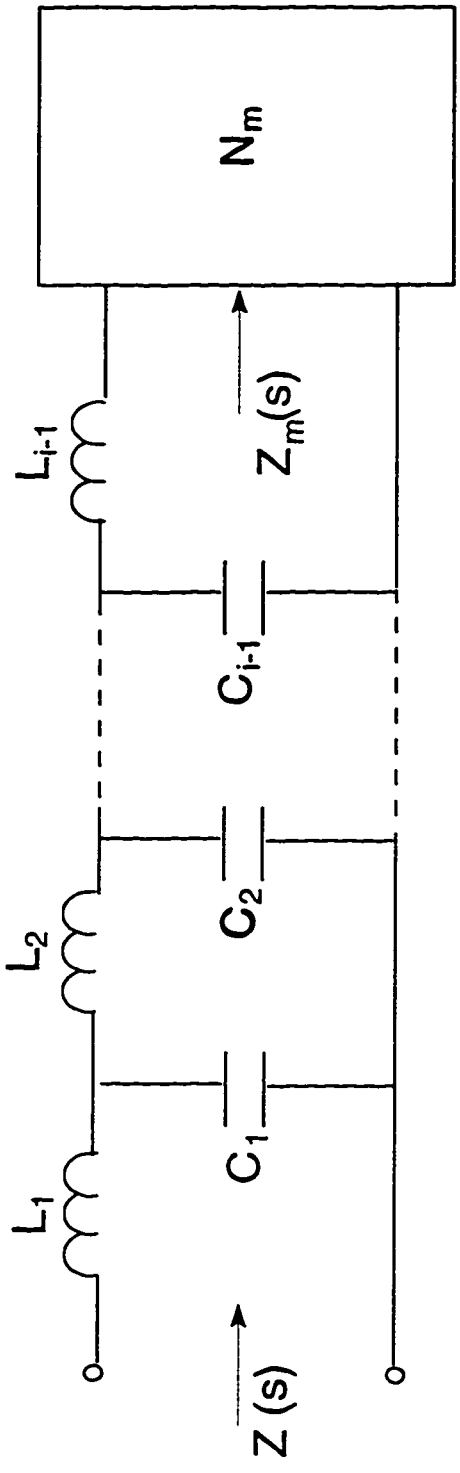

Figure 2.9: Brune Preamble [4].

whose transmission matrix is

$$\frac{1}{f(s)}\begin{pmatrix} A_1 & B_1 \\ C_1 & D_1 \end{pmatrix} \tag{2.46}$$

where $f(s)$ is the product of the transmission zeros to be extracted, the driving point impedance $Z_{m1}(s)$ of the remaining network is

$$Z_{m1}(s) = \frac{D_1 Z_m(s) - B_1}{A_1 - C_1 Z_m(s)} \tag{2.47}$$

If s_0 is a simple zero of $Z_m(s) + Z_m(-s)$, then $Z_m(s)$ is augmented as follows

$$Z_m(s) = \frac{(m_1 + n_1)G}{(m_2 + n_2)G} = \frac{M_1 + N_1}{M_2 + N_2} \tag{2.48}$$

where G contains all the left hand zeros in $Re\{s < 0\}$ of odd multiplicity and the functions m_1, m_2, n_1, n_2 are replaced with M_1, M_2, N_1, N_2. The extraction of zero sections in cascade is repeated until all the zeros of transmission are realized, and we reach an impedance whose value equals the terminating resistor.

Depending on the location of the zeros of transmission in the s-plane, three types of zero section are needed. The first realizes a pair of conjugate jw-axis zeros, the second realizes a pair of zeros on the real axis, and the third realizes a complex conjugate quadruplet of zeros.

1. Transmission Zeros at Real Frequencies Transmission zeros at real frequencies of the form of $s^2 = -w_0{}^2$ are extracted by the Brune section, whose transmission matrix is given by

$$\frac{1}{\left(1+\frac{s^2}{w_0{}^2}\right)}\begin{pmatrix} 1+as^2 & bs \\ cs & 1+ds^2 \end{pmatrix} \tag{2.49}$$

where a, b, c, and d are constants. For $Z_m(jw_0) = jX(w_0)$, and $Z'_m(jw_0) = X'(w_0)$, where $Z'_m(s) = \frac{d}{ds}Z_m(s)$. The constants a, b, c and d are given by the expressions [15]

$$\begin{aligned} a &= \frac{w_0X'(w_0)+X(w_0)}{w_0{}^2\{w_0X'(w_0)-X(w_0)\}} \\ c &= \frac{2}{w_0\{w_0X'(w_0)-X(w_0)\}} \\ d &= \frac{1}{aw_0{}^4} \\ b &= \frac{1}{c}\left(a+d-\frac{2}{w_0{}^2}\right) \end{aligned} \tag{2.50}$$

and equation (2.51) yield the element values for the circuit in figure (2.10) as [15]

$$C = \frac{2}{w_0\{w_0X'(w_0)-X(w_0)\}} \tag{2.51}$$

$$L_1 = \frac{w_0X'(w_0)+X(w_0)}{2w_0} \tag{2.52}$$

$$L_2 = \frac{\{w_0 X'(w_0) - X(w_0)\}^2}{2w_0\{w_0 X'(w_0) + X(w_0)\}} \tag{2.53}$$

$$M = \frac{\{w_0 X'(w_0) - X(w_0)\}}{2w_0}$$

$$= \sqrt{L_1 L_2} \tag{2.54}$$

It can be proved that the values L_1, L_2, C and M are all guaranteed positive [4].

2. Transmission Zeros on Real Axis Transmission zeros on the real axis of the form of $s^2 = \pm\sigma_0$ are extracted by the C section whose transmission matrix is

$$\frac{1}{\left(1 - \frac{s^2}{\sigma^2}\right)} \begin{pmatrix} 1 + as^2 & bs \\ cs & 1 + ds^2 \end{pmatrix} \tag{2.55}$$

where the constants a, b, c, d are [15]

$$a = \frac{\sigma_0 Z'(\sigma_0) + Z(\sigma_0)}{\sigma_0{}^2\{Z(\sigma_0) - \sigma_0 Z'(\sigma_0)\}}$$

$$c = \frac{2}{\sigma_0\{Z(\sigma_0) - \sigma_0 Z'(\sigma_0)\}}$$

$$d = \frac{1}{a\sigma_0{}^4}$$

$$b = \frac{1}{c}\left(a + d + \frac{2}{\sigma_0{}^2}\right) \tag{2.56}$$

The resulting element values of the circuit of figure (2.10) are

$$L_1 = \frac{Z(\sigma_0) + \sigma_0 Z'(\sigma_0)}{2\sigma_0} \tag{2.57}$$

$$L_2 = \frac{\{Z(\sigma_0) - \sigma_0 Z'(\sigma_0)\}^2}{2\sigma_0\{Z(\sigma_0) + \sigma_0 Z'(\sigma_0)\}} \tag{2.58}$$

$$M = -\frac{\{Z(\sigma_0) - \sigma_0 Z'(\sigma_0)\}}{2\sigma_0} \tag{2.59}$$

$$C = \frac{2}{\sigma_0\{Z(\sigma_0) - \sigma_0 Z'(\sigma_0)\}} \tag{2.60}$$

It can be proved that the values L_1, L_2, and C are all positive and the mutual inductance M is negative in this case [4].

3. Complex Transmission Zeros Complex transmission zeros of the form of $|s_0|^2 = {\sigma_0}^2 + {w_0}^2$ are extracted by the D section with the transmission matrix

$$\frac{1}{\{s^4 2({w_0}^2 - {\sigma_0}^2) + |s_0|^4\}} \begin{pmatrix} |s_0|^4 + a_1 s^2 + a_2 s^4 & s(b_1 + b_2 s^2) \\ s(c_1 + c_2 s^2) & |s_0|^4 + d_1 s^2 + d_2 s^4 \end{pmatrix} \tag{2.61}$$

The constants a_1, a_2, c_1, c_2 are found as [15]

$$a_1 = 2({w_0}^2 - {\sigma_0}^2) + 4H_1 H_2 \tag{2.62}$$

$$a_2 = 1 + 4H_2\{I_1(X\sigma_0 + Rw_0) + I_2(X\sigma_0 - Rw_0)\} \tag{2.63}$$

$$c_1 = 8\sigma_0 w_0({\sigma_0}^2 + {w_0}^2) I_2 H_2 \tag{2.64}$$

$$c_2 = 8\sigma_0 w_0 I_1 H_2 \tag{2.65}$$

where

$$I_1 = X\sigma_0{}^3 - R'\sigma_0 w_0(\sigma_0{}^2 + w_0{}^2) + Rw_0{}^3 \quad (2.66)$$

$$I_2 = -X\sigma_0{}^3 + R'\sigma_0 w_0(\sigma_0{}^2 - w_0{}^2) - 2X'\sigma_0{}^2 w_0{}^2 + Rw_0{}^3 \quad (2.67)$$

$$I_3 = X'(\sigma_{02} + w_0{}^2) + 3w_0 R - 3\sigma_0 X \quad (2.68)$$

$$I_4 = -X'(\sigma_{02} - w_0{}^2) - 2\sigma_0 w_0 R' + w_0 R + \sigma_0 X \quad (2.69)$$

$$H_1 = I_2\{X\sigma_0(3w_0{}^2 - \sigma_0{}^2) + Rw_0(3w_0{}^2 - \sigma_0{}^2)\} + I_1(\sigma_0{}^2 + w_0{}^2)(Rw_0 - X\sigma_0) \quad (2.70)$$

$$H_2 = 1/(I_2 I_3 - I_1 I_4) \quad (2.71)$$

$$Z(s_0) = R + jX \quad (2.72)$$

$$Z'(s_0) = R' + jX' \quad (2.73)$$

The b and d parameters are obtained from the corresponding c and a parameters if $Z(s_0) = R + jX$ is replaced by $Y(s_0) = G + jB$, and $Z'(s_0) = R' + jX'$ is replaced by $Y'(s_0) = G' + jB'$.

A realization based on the impedance matrix is shown in figure (2.11) with the element values given by [15]

$$M_1 = 1/c_2 \quad (2.74)$$

$$L_1 = a_2/c_2 \quad (2.75)$$

$$L_2 = M_1{}^2/L_1 \tag{2.76}$$

$$M_2 = \frac{-1}{c_1{}^2 c_2}\{c_1{}^2 - 2(w_0 - \sigma_0{}^2)c_1 c_2 + |s_0|^4 c_2{}^2\} \tag{2.77}$$

$$L_3 = \frac{1}{c_1{}^2 c_2}(a_1 c_1 c_2 - a_2 c_1{}^2 - |s_0|^4 c_2{}^2) \tag{2.78}$$

$$L_4 = M_2{}^2/L_3 \tag{2.79}$$

$$C_a = c_2/(c_1 L_3) \tag{2.80}$$

$$C_b = c_1/|s_0|^4 \tag{2.81}$$

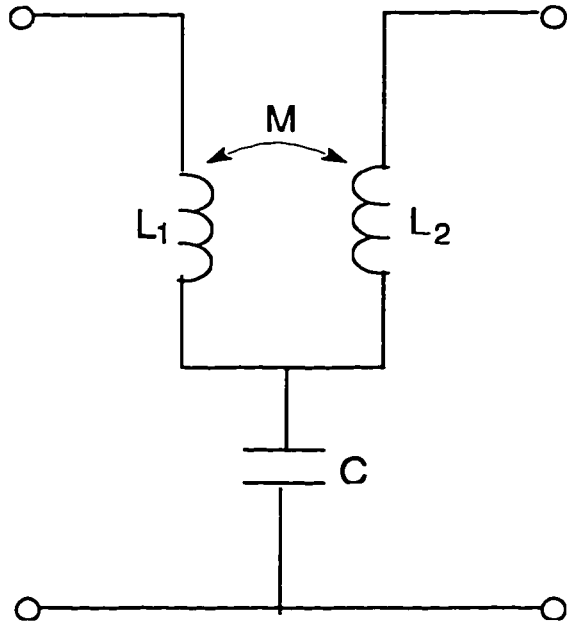

Figure 2.10: Brune Section ($M > 0$) or C Section ($M < 0$) [4]

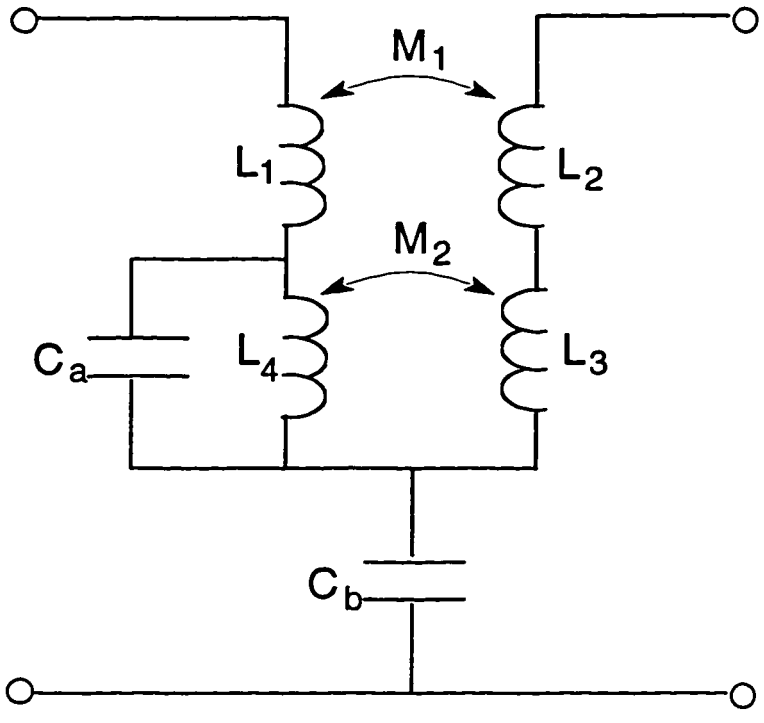

Figure 2.11: D section realized from impedance synthesis [4]

2.5 Problem statement

From the above discussion, we see that there exist a large number of useful solutions for the design of data transmission filters. Researchers have adopted different methods of formulation to obtain better amplitude and phase characteristics. However, the optimum solution to the combined amplitude and phase problem has not yet been found. Also, the evaluation parameters stated in section (1.3) vary considerably with the technique used for the filter design.

Also, all the above solutions do not address the problem of designing a rapidly decaying impulse response which may be quite useful in data transmission filters. This characteristic is extremely important for the proper performance of a communication channel as it is expected to give better sampling error and smaller side lobe amplitudes of the pulses, thereby helpful in controlling intersymbol interference and excessive jittering effects. Some good theoretical work in the design of these kind of pulse shapes has been done by Tugbay [14] and Hassan[10] but their work does not produce a design procedure to obtain realizable filter transfer functions.

Therefore, it is the objective of this thesis to design data transmission filters with a rapidly decaying time response by maximizing the energy in the main lobe of the pulse. In this manner, very little energy will creep outside the band $-T < t < T$ and hence minimizing both the ISI and the error accumulation due to jittering problem. The procedure follows the theory proposed earlier in [14] and [10] but applied directly

to the proposed filter transfer function with unknown coefficients. The proposed technique relies on the concepts given in reference [1] and uses its modelled transfer function as the starting point. Optimal coefficients are obtained and the actual filter parameters are readily available. This problem is being addressed in the following chapters.

Chapter 3

Proposed Filter Design

In this chapter, the proposed design of the Nyquist type data transmission filter is presented. The theory of the proposed filter is first stated in section 3.1. This is followed by the model description of the filter in section 3.2. The design of the impulse response of the Nyquist filter is explained in section 3.3. This design procedure is extended to the practical case of pulse input in section 3.4. The proposed method represents a modification of that in reference [1] by optimizing the energy instead of imposing constraints on the real part of the filter transfer function.

3.1 Theory

A Nyquist pulse shape filter is designed with energy maximized within the main lobe (-T, T) of the impulse response. In our approach, we design the pulse

such that energy can be maximized in any time period $(-\sigma T, \sigma T)$ where σ is any non-zero positive real number. We first start by assuming a rational function to represent the transfer function of the filter. The starting point is the same as that in reference [1], namely a transfer function with close approximation to the linear phase characteristics. The numerator of the transfer function contains only even powers of s. Hence the resulting phase of the filter is the reciprocal of the phase of the linear phase polynomial. The design involves the determination of the numerator coefficients of the filter transfer function to meet the required specifications. The resulting filter is restricted to a low pass type.

The order of numerator of the transfer function to be designed is first selected. The magnitude of the filter transfer function is expressed in terms of the unknown numerator coefficients $a_i's$ and so are the selected time domain energy $E(\sigma T)$ in the interval $(-\sigma T, \sigma T)$ and the total energy $E(\infty)$. The process involves determination of the numerator coefficients $a_i's$ by minimizing the difference $J = E(\sigma T) - \lambda E(\infty)$, where λ is the ratio of the two energies.

The methodology will also incorporate the Nyquist condition to force all residual tails of the received pulses to be zero. Such design is important in minimizing timing errors at the sampling time at the receiver. The numerator coefficients are determined using these two conditions of energy maximization and Nyquist criteria.

3.2 Model Description.

Let the filter transfer function be of the form

$$H(s) = \frac{P_m(s)}{Q_n(s)} \qquad m < n \tag{3.1}$$

with

$$P_m(s) = \sum_{i=1}^{m} a_i s^{2(i-1)} \tag{3.2}$$

where $s = \sigma + jw$ is the usual complex frequency. $P_m(s)$ is an even polynomial of order m for a reciprocal realization of $H(s)$ and $Q_n(s)$ is the any polynomial of degree n which is strictly Hurwitzian. The transfer function has the same form as in reference [1] with the denominator as the equidistant linear phase polynomial. The filter transfer function of this form will be referred to as Model I functions.

Depending on whether n is odd or even, m is chosen as

$$m = \frac{n}{2} \qquad \text{for n even} \tag{3.3}$$

$$m = \frac{n+1}{2} \qquad \text{for n odd} \tag{3.4}$$

Replacing s by jw in equation (3.1), we may write

$$H(jw) = \frac{P_m(jw)}{Q_n(jw)} \tag{3.5}$$

with

$$P_m(jw) = \sum_{i=1}^{m} (-1)^{i-1} a_i . w^{2(i-1)} \tag{3.6}$$

Also, $Q_n(jw)$ may be written as

$$Q_n(jw) = |Q_n(jw)| \angle \phi(w) \tag{3.7}$$

The magnitude of the filter transfer function, $|H(jw)|$ is therefore

$$|H(jw)| = \frac{\sum_{i=1}^{m} (-1)^{i-1} a_i . w^{2(i-1)}}{|Q_n(jw)|} \tag{3.8}$$

The impulse response $h(t)$ of the filter is found by taking the Fourier transform of $H(jw)$ such that

$$\begin{aligned} h(t) &= \frac{1}{2\pi} \int_{-2w_0}^{2w_0} |H(jw)| . e^{-j\beta w} . e^{jwt} . dw \\ &= \frac{1}{2\pi} \int_{-2w_0}^{2w_0} |H(jw)| . e^{jw(t-\beta)} . dw \\ &= \frac{1}{2\pi} \left[\int_{-2w_0}^{0} |H(jw)| . e^{jw(t-\beta)} . dw + \int_{0}^{2w_0} |H(jw)| . e^{jw(t-\beta)} . dw \right] \end{aligned} \tag{3.9}$$

Substituting $w = -w$ in the first integral and since $|H(-jw)| = |H(jw)|$,

$$\begin{aligned} h(t) &= \frac{1}{2\pi}\left[\int_0^{2w_0} |H(jw)|.e^{-jw(t-\beta)}.dw + \int_0^{2w_0} |H(jw)|.e^{jw(t-\beta)}.dw\right] \\ &= \frac{1}{2\pi}\int_0^{2w_0} |H(jw)|.Cos[w(t-\beta)].dw \end{aligned} \tag{3.10}$$

Incorporating equation (3.8) in the equation (3.10), we have

$$h(t) = \frac{1}{2\pi}\int_0^{2w_0} \frac{\sum_{i=1}^{m}(-1)^{i-1}a_i.w^{2(i-1)}.Cos[w(t-\beta)]}{|Q_n(jw)|}.dw \tag{3.11}$$

The time domain energy in the interval $(\beta - \delta 1)$ to $(\beta + \delta 2)$ is given by

$$E(\sigma T) = \int_{\beta-\delta 1}^{\beta+\delta 2} h^2(t).dt \tag{3.12}$$

where and $\delta 1$ and $\delta 2$ are any two real positive parameters. Using equation (3.11), $E(\sigma T)$ can be represented in terms of the numerator coefficients $a_i's$ as

$$E(\sigma T) = \int_{\beta+\delta 1}^{\beta-\delta 2}\left[\frac{1}{2\pi}\int_0^{2w_0} \frac{\sum_{i=1}^{m}(-1)^{i-1}a_i.w^{2(i-1)}Cos[w(t-\beta)]}{|Q_n(jw)|}dw\right]^2 dt \tag{3.13}$$

Similarly the energy in the frequency domain is given by

$$E(\infty) = \frac{1}{2\pi}\int_{-2w_0}^{2w_0} |H(jw)|^2.dw \qquad (3.14)$$
$$= \frac{1}{\pi}\int_{0}^{2w_0} \left[\frac{\sum_{i=1}^{m}(-1)^{i-1}a_i.w^{2(i-1)}}{|Q_n(jw)|}\right]^2 dw$$

3.3 Design for Impulse Input

In order to maximize the energy in the major lobe or within any period of time, we minimize the quantity J where

$$J = E(\sigma T) - \lambda.E(\infty) \qquad (3.15)$$

where λ is a constant and $E(\sigma T)$ and $E(\infty)$ are the energies as derived in section (3.2).

Applying the Nyquist criteria to the design, we incorporate the condition [16]

$$|H[j(w_0 - w)]| + |H[j(w_0 + w)]| = C \qquad (3.16)$$

where C is a constant and w_0 is the Nyquist frequency such that $0 \leq w \leq w_0$.

Incorporating equation (3.16) in equation (3.15), we get

$$J = E(\sigma T) - \lambda E(\infty) + \eta_r\{|H[j(w_0 - w_r)]| + |H[j(w_0 + w_r)]| - C\} \qquad (3.17)$$

where η_r is a set of lagrange multipliers and $0 \leq w_r \leq w_0$. Differentiating J w.r.t. $a_i's$ and equating the result to zero, we get the solution in the form of

$$\sum_{i=1}^{m} a_i.[X_{(i,k)} - \lambda.Z_{(i,k)}] + \sum_{r=1}^{R} \eta_r.Y_{(k,r)} = 0 \tag{3.18}$$

where

$$X_{(i,k)} = \frac{2}{\pi^2} \int_{\beta-\delta 1}^{\beta+\delta 2} X1_i(t) \times X1_k(t).dt \tag{3.19}$$

$$X1_i(t) = \int_0^{2w_0} f_i(w,t).dw \tag{3.20}$$

$$f_i(w,t) = \frac{(-1)^{i-1} w^{2(i-1)}.Cos[w(t-\beta)]}{|Q_n(jw)|} \tag{3.21}$$

$$Y_{(i,r)} = U_{(i,r)} + S_{(i,r)} \tag{3.22}$$

$$U_{(i,r)} = \frac{(-1)^{i-1}(w_0 - w_r)^{2(i-1)}}{|Q_n[j(w_0 - w_r)]|} \tag{3.23}$$

$$S_{(i,r)} = \frac{(-1)^{i-1}(w_0 + w_r)^{2(i-1)}}{|Q_n[j(w_0 + w_r)]|} \tag{3.24}$$

and

$$Z_{(i,k)} = \frac{2}{\pi} \int_0^{2w_0} G_i(w) \times G_k(w).dw \tag{3.25}$$

$$G_i(w) = \frac{(-1)^{i-1} w^{2(i-1)}}{|Q_n(jw)|} \tag{3.26}$$

where $i, k = 1, 2, ...m$ and R is any convenient number of frequencies w_r in the range 0 to w_0.

Also, equation (3.16) can be written as

$$\sum_{i=1}^{m} a_i.Y_{(i,r)} = C \tag{3.27}$$

for $r = 1, 2, ..., R$.

Equations (3.18) and (3.27) can be written in matrix form as

$$\begin{bmatrix} x_{11}-\lambda z_{11} & \cdots & .. & x_{m1}-\lambda z_{m1} & y_{11} & y_{12} & .. & y_{1R} \\ x_{12}-\lambda z_{12} & \cdots & .. & x_{m2}-\lambda z_{m2} & y_{21} & y_{22} & .. & y_{2R} \\ \cdots & \cdots & .. & \cdots & \cdots & .. & .. & \cdots \\ \cdots & \cdots & .. & \cdots & \cdots & .. & .. & \cdots \\ x_{1m}-\lambda z_{1m} & \cdots & .. & x_{mm}-\lambda z_{mm} & y_{m1} & y_{m2} & .. & y_{mR} \\ y_{11} & y_{21} & .. & y_{m1} & 0 & 0 & .. & 0 \\ y_{12} & y_{22} & .. & y_{m2} & 0 & 0 & .. & 0 \\ \cdots & \cdots & .. & \cdots & \cdots & \cdots & .. & .. \\ y_{1R} & \cdots & .. & y_{mR} & 0 & 0 & .. & 0 \end{bmatrix} \cdot \begin{bmatrix} a_1 \\ a_2 \\ : \\ : \\ a_m \\ \eta_1 \\ \eta_2 \\ : \\ \eta_R \end{bmatrix} = \begin{bmatrix} 0 \\ 0 \\ : \\ : \\ 0 \\ C \\ C \\ : \\ C \end{bmatrix} \tag{3.28}$$

$$A = \left[\frac{a_i}{\eta_r}\right] = inv[X].\left[\frac{0}{C}\right] \tag{3.29}$$

The constants $a_i's$ are determined for a particular λ in terms of C by taking the first n terms of the column vector A. This completes the solution of the transfer function with the required energy in the main lobe of the pulse. Once the transfer function is found the energy ratio in the frequency domain can be found as through the condition

$$\{|H[j(w_0 - w)]| + |H[j(w_0 + w)]|\}^2 = C^2 \tag{3.30}$$

$$|H[j(w_0 - w)]|^2 + |H[j(w_0 + w)]|^2 + 2|H[j(w_0 - w)]||H[j(w_0 + w)]| = C^2$$

Integrating w.r.t w between 0 and w_0, we get

$$E_0 + \int_0^{w_0} 2|H[j(w_0 - w)]||H[j(w_0 + w)]|dw = C^2.w_0 \tag{3.31}$$

where

$$E_0 = \int_0^{w_0} |H[j(w_0 - w)]|^2 dw + \int_0^{w_0} |H[j(w_0 + w)]|^2 dw \tag{3.32}$$

$$E_R = \frac{E_0}{C^2.w_0} = 1 - \int_0^{w_0} \frac{2}{C^2.w_0} |H[j(w_0 - w)]||H[j(w_0 + w)]|dw \tag{3.33}$$

E_R is the ratio of energy in the frequency domain and the maximum energy $C^2 w_0$. The energy ratio in the frequency domain, E_0 can be found with the help of $a_i's$.

For a given set of $a_i's$, we expect the energy ratio E_R to be less than one. We also expect that as this ratio increases, the energy in the side lobes of the pulses increases. According to the specifications and requirements, a suitable combination of the two ratios λ and E_R may be chosen. For maximum energy in the time domain pulse response, we select the maximum λ satisfying the condition $E_R < 1$.

3.4 Design for Pulse Input

In this section, the design of impulse input is extended to the practical case of pulse input as impulses cannot be generated. Hence a pulse of time duration T as an input is a more feasible case. The extension to pulse inputs is based on the concepts given in [1]. The transfer function $H(s)$ of the filter is represented as the product of two functions as [1]

$$H(s) = H_p(s) \times P(s) \tag{3.34}$$

where $P(s)$ is the Laplace transform of the pulse $p(t)$ and $H_p(s)$ is the transfer function to be designed for pulse input. Then, the impulse response of the filter with transfer function $H(s)$ is the same as the pulse response of the filter with transfer function $H_p(s)$.

The pulse $p(t)$ of duration T can be written as

$$p(t) = u(t) - u(t - T) \tag{3.35}$$

where $u(t)$ is the unit step function and T is the baud rate given by $T = \pi/w_0$. The Laplace transform of the above pulse is found to be [1]

$$P(s) = \frac{1}{s}(1 - e^{-sT}) \tag{3.36}$$

and its respective spectrum as

$$P(jw) = \frac{2}{w} Sin(\frac{T}{2}w) \exp(-j\frac{T}{2}w) \tag{3.37}$$

We see from equations (3.16) and (3.34) that the Nyquist condition can be represented as

$$|H_p[j(w_0 - w)]||P[j(w_0 - w)]| + |H_p[j(w_0 + w)]||P[j(w_0 + w)]| = C \tag{3.38}$$

where C is a constant and $0 \leq w \leq w_0$.

If we model the filter transfer function $H_p(jw)$ to be of the form

$$H_p(jw) = \frac{\sum_{i=1}^{m}(-1)^{i-1}A_i.w^{2(i-1)}}{|Q_n(jw)|\angle\phi(w)} \tag{3.39}$$

we see that

$$Arg\{H(jw)\} = Arg\{H_p(jw)\} + Arg\{P(jw)\} \tag{3.40}$$

interpolate the function $(\beta + T/2)w$ at n+1 equidistant points, satisfying the condition

$(\beta + \frac{T}{2}).w_i - Arg\{H(jw_i)\} = 0 \qquad w_i = i\alpha \quad for$ i=0,1,2,.....,n

Using equation (3.11), the energy in the required region in the time domain is given by

$$E(\sigma T) = \int_{\beta-\delta 1}^{\beta+\delta 2} \left[\frac{1}{2\pi} \int_0^{2w_0} \frac{\sum_{i=1}^{m} (-1)^{i-1} A_i . w^{2(i-1)} Cos[w(t-\beta)]}{|X_n(jw)|} dw \right]^2 dt \qquad (3.41)$$

where

$$|X_n(jw)| = \frac{|Q_n(jw)|}{P_n(jw)}$$

and $\delta 1$ and $\delta 2$ are any two parameters defining the energy maximization interval. Similarly, using equation (3.14), the energy in the frequency domain is given by

$$E(\infty) = \frac{1}{\pi} \int_0^{2w_0} \left[\frac{\sum_{i=1}^{m} (-1)^{i-1} A_i . w^{2(i-1)}}{|X_n(jw)|} \right]^2 dw \qquad (3.42)$$

Substituting the respective terms in the equation (3.17) and differentiating J w.r.t. A_i's and equating the result to zero, we get the solution in the form of

$$\sum_{i=1}^{m} A_i . [X'_{(i,k)} + \lambda . Z'_{(i,k)}] + \sum_{r=1}^{R} \eta_r . Y'_{(k,r)} = 0 \qquad (3.43)$$

where

$$X'_{(i,k)} = \frac{2}{\pi^2} \int_{\beta-\delta 1}^{\beta+\delta 2} X2_i(t) \times X2_k(t) . dt \qquad (3.44)$$

$$X2_i(t) = \int_0^{2w_0} f_i'(w,t).dw \tag{3.45}$$

$$f_i'(w,t) = \frac{(-1)^{i-1}w^{2(i-1)}.Cos[w(t-\beta)]}{|X_n(jw)|} \tag{3.46}$$

$$Y'_{(i,r)} = U'_{(i,r)} + S'_{(i,r)} \tag{3.47}$$

$$U'_{(i,r)} = \frac{|P[j(w_0 - w_r)]|(-1)^{i-1}(w_0 - w_r)^{2(i-1)}}{|Q_n[j(w_0 - w_r)]|} \tag{3.48}$$

$$S'_{(i,r)} = \frac{|P[j(w_0 + w_r)]|(-1)^{i-1}(w_0 + w)^{2(i-1)}}{|Q_n[j(w_0 + w_r)]|} \tag{3.49}$$

$$Z'_{(i,k)} = \frac{2}{\pi}\int_0^{2w_0} G_i'(w) \times G_k'(w).dw \tag{3.50}$$

$$G_i'(w) = \frac{(-1)^{i-1}w^{2(i-1)}}{|X_n(jw)|} \tag{3.51}$$

Also, equation (3.16) can be written as

$$\sum_{i=1}^{m} A_i.Y'_{(i,r)} = C \tag{3.52}$$

where $r = 1, 2, ..., R$.

Equations (3.43) and (3.52) can be written in a similar matrix form as shown in equation (3.28) and the unknown numerator coefficients $A_i's$ are found out. Subsequently a network can be synthesized for the designed filter transfer function using available techniques outlined in section (2.4).

Chapter 4

Phase and Energy Optimization

In this chapter, we will study the feasibility of simultaneous optimization of both energy and phase of the filter transfer function. The phase of the filter which was set to that of the equidistant linear phase polynomial is further optimized by choosing the numerator of filter transfer function as a general order polynomial of s. The additional odd function coefficients of the numerator are used to reduce the linear phase error of the filter. However the use of general polynomial of s in the numerator will require additional elements in the filter realization or an active realization is needed. Therefore a performance comparison based on the equal number of elements has to be made with Model I functions before using these transfer functions.

4.1 Model Description

For the filter transfer function of the form

$$H(s) = \frac{P_m(s)}{Q_n(s)} \qquad m < n \tag{4.1}$$

we choose $P_m(s)$ such that

$$P_m(s) = \sum_{i=1}^{m} a_i s^{2(i-1)} + \sum_{i=1}^{m1} b_{i.} s^{2i-1} \tag{4.2}$$

The filter transfer functions of the above form will be referred as Model II.

Depending upon whether n is even or odd,

$$m = \frac{n}{2} \quad \text{and} \quad m1 = \frac{n}{2} \quad \text{for n=even} \tag{4.3}$$

and

$$m = \frac{n+1}{2} \quad \text{and} \quad m1 = \frac{n-1}{2} \quad \text{for n=odd} \tag{4.4}$$

Since $Q_n(s)$ is the linear phase polynomial which is strictly Hurwitz, we can write equation (4.1) as

$$|H(jw)|\angle -\beta w = \frac{\sum_{i=1}^{m}(-1)^{i-1} a_i w^{2(i-1)} + j\sum_{i=1}^{m1}(-1)^{i+1} b_{i.} w^{2i-1}}{|Q_n(jw)|.\angle\phi(w)} \tag{4.5}$$

where $j = \sqrt{-1}$.

We see that the numerator is divided as the sum of the odd and even powers of w with unknown coefficients $a_i's$ and $b_i's$. Therefore, the only unknown in the filter transfer function are the $a_i's$ and $b_i's$. These unknowns are determined such that the time domain pulse has maximum energy in its main lobe and also satisfies Nyquist criterion.

By dividing $H(jw)$ into real and imaginary parts, we get

$$|H(jw)|Cos[\phi(w) - \beta w] = \frac{\sum_{i=1}^{m}(-1)^{i-1}a_i w^{2(i-1)}}{|Q_n(jw)|} \tag{4.6}$$

$$|H(jw)|Sin[\phi(w) - \beta w] = \frac{\sum_{i=1}^{m1}(-1)^{i+1}b_i w^{2i-1}}{|Q_n(jw)|} \tag{4.7}$$

The impulse response of the filter is found in terms of the coefficients $a_i's$ using equations (3.10) and equation (4.6) as

$$\begin{aligned} h(t) &= \frac{1}{2\pi}\int_0^{2w_0} |H(jw)|.Cos[w(t-\beta)].dw \\ &= \frac{1}{2\pi}\int_0^{2w_0} \frac{\sum_{i=1}^{m}(-1)^{i-1}a_i w^{2(i-1)}.Cos[w(t-\beta)]}{|Q_n(jw)|.Cos[\phi(w)-\beta w]}.dw \end{aligned} \tag{4.8}$$

The energy in the required region of $(\beta - \delta 1)$ and $(\beta + \delta 2)$ in the time domain for Model II is given by

$$E(\sigma T) = \int_{\beta-\delta 1}^{\beta+\delta 2} h^2(t).dt \tag{4.9}$$
$$= \int_{\beta-\delta 1}^{\beta+\delta 2} \left[\frac{1}{2\pi}\int_0^{2w_0} \frac{\sum_{i=1}^{m}(-1)^{i-1}a_{i.}w^{2(i-1)}Cos[w(t-\beta)]}{|Q_n(jw)|Cos\,[\phi(w)-\beta w]}dw\right]^2 dt$$

where and $\delta 1$ and $\delta 2$ are any two real positive parameters. Similarly the energy in the frequency domain is given by

$$E(\infty) = \frac{1}{2\pi}\int_{-2w_0}^{2w_0} |H(jw)|^2.dw \tag{4.10}$$
$$= \frac{1}{\pi}\int_0^{2w_0} \left[\frac{\sum_{i=1}^{m}(-1)^{i-1}a_{i.}w^{2(i-1)}}{|Q_n(jw)|Cos[\phi(w)-\beta w]}\right]^2 dw$$

4.2 Design for Impulse Input

For the numerator polynomial of the general form, we maximize the energy in the major lobe or within any specified interval by minimizing the equation (3.15). Also, using equation (4.6) the Nyquist condition is expressed in the form of equation (3.16), where

$$|H[j(w_0-w)]| = \frac{\sum_{i=1}^{m}(-1)^{i-1}a_i(w_0-w)^{2(i-1)}}{|Q_n[j(w_0-w)]|Cos[\phi(w_0-w)-\beta(w_0-w)]} \tag{4.11}$$

and

$$|H[j(w_0+w)]| = \frac{\sum_{i=1}^{m}(-1)^{i-1}a_i(w_0+w)^{2(i-1)}}{|Q_n[j(w_0+w)]|Cos[\phi(w_0+w)-\beta(w_0+w)]} \tag{4.12}$$

Incorporating the two conditions, we minimize equation (3.17) to obtain the solution in form of equation (3.18), where

$$X_{(i,k)} = \frac{2}{\pi^2}\int_{\beta-\delta 1}^{\beta+\delta 2} X3_i(t) \times X3_k(t).dt \tag{4.13}$$

$$X3_i(t) = \int_0^{2w_0} F_i(w,t).dw \tag{4.14}$$

$$F_i(w,t) = \frac{(-1)^{i-1}w^{2(i-1)}}{|Q_n(jw)|Cos[\phi(w)-\beta w]} \tag{4.15}$$

$$Y_{(i,r)} = V_{(i,r)} + T_{(i,r)} \tag{4.16}$$

$$V_{(i,r)} = \frac{(-1)^{i-1}(w_0-w_r)^{2(i-1)}}{|Q_n[j(w_0-w_r)]|.Cos[\phi(w_0-w)-\beta(w_0-w)]} \tag{4.17}$$

$$T_{(i,r)} = \frac{(-1)^{i-1}(w_0+w_r)^{2(i-1)}}{|Q_n[j(w_0+w_r)]|.Cos[\phi(w_0+w)-\beta(w_0+w)]} \tag{4.18}$$

$$Z_{(i,k)} = \frac{2}{\pi}\int_0^{2w_0} I_i(w) \times I_k(w).dw \tag{4.19}$$

$$I_i(w) = \frac{(-1)^{i-1}w^{2(i-1)}}{|Q_n(jw)|Cos[\phi(w) - \beta w]} \tag{4.20}$$

where $i, k = 1, 2, ...m$ and R depends on the how much we divide w in equation (3.16)

Also, the Nyquist condition is written as in equation (3.27). The above equations are incorporated to give the solution in matrix form similar to the one shown in equation (3.28) through which the the coefficients $a_i's$ are found.

Once $a_i's$ are determined, then one may use equations (4.6) and (4.7) to write

$$\frac{\sum_{i=1}^{m}(-1)^{i-1}a_{i.}w^{2(i-1)}}{|Q_n(jw)|Cos[\phi(w) - \beta w]} = \frac{\sum_{i=1}^{m1}(-1)^{i+1}b_{i.}w^{2i-1}}{|Q_n(jw)|Sin[\phi(w) - \beta w]} \tag{4.21}$$

or

$$\left[\sum_{i=1}^{m1}(-1)^{i+1}b_i w^{2i-1} - H_a(w)\right]^2 = \epsilon^2 \tag{4.22}$$

where

$$H_a(w) = \sum_{i=1}^{m}(-1)^{i-1}a_{i.}w^{2(i-1)}Tan[\phi(w) - \beta w]$$

The right hand side of equation (4.22), ϵ^2 is an error term. Integrating equation (4.22) between 0 and $2w_0$ gives the total error within the full band of $2w_0$. To

minimize this error, we differentiate with respect to $b_i's$ and set the result to zero. This gives

$$b_i = inv(M1) \times N1 \tag{4.23}$$

where

$$M1 = \frac{(-1)^{i+k+2}(2w_0)^{(2i+2k-1)}}{2i+2k-1} \tag{4.24}$$

and

$$N1 = \int_0^{2w_0} (-1)^{k+1} H_a(w) w^{2k-1}.dw \tag{4.25}$$

4.3 Design for Pulse Input

The design of impulse response may be extended to that for pulse input using the same theory as provided in section (3.4). This is very important application since the real life input to the filter is a pulse and not an impulse. For the numerator of the general form having both even and odd polynomial terms, we model the transfer function as

$$H_p(jw) = \frac{\sum_{i=1}^{m}(-1)^{i-1}A_{i.}w^{2(i-1)} + j\sum_{i=1}^{m1}(-1)^{i+1}B_{i.}w^{2i-1}}{|Q_n(jw)|\,\angle\phi(w)} \tag{4.26}$$

where $j = \sqrt{-1}$ and hence

$$|H_p(jw)|Cos[\phi(w) - (\beta + T/2)w] = \frac{\sum_{i=1}^{m}(-1)^{i-1}A_{i.}w^{2(i-1)}}{|Q_n(jw)|} \tag{4.27}$$

$$|H_p(jw)|Sin[\phi(w) - (\beta + T/2)w] = \frac{\sum_{i=1}^{m1}(-1)^{i+1}B_{i.}w^{2i-1}}{|Q_n(jw)|} \tag{4.28}$$

Using equation (3.12), the energy in the region $(\beta - \delta 1)$ to $(\beta + \delta 2)$ of time domain is given by

$$E(\sigma T) = \int_{\beta-\delta 1}^{\beta+\delta 2}\left[\frac{1}{2\pi}\int_0^{2w_0}\frac{\sum_{i=1}^{m}(-1)^{i-1}A_{i.}w^{2(i-1)}Cos[w(t-\beta)]}{|X_n(jw)|\,Cos[\phi(w) - (\beta + T/2)w]}dw\right]^2 dt \tag{4.29}$$

where and $\delta 1$ and $\delta 2$ are any two parameters. Similarly using equation (3.14), the energy in the frequency domain is given by

$$E(\infty) = \frac{1}{\pi}\int_0^{2w_0}\left[\frac{\sum_{i=1}^{m}(-1)^{i-1}A_{i.}w^{2(i-1)}Cos[w(t-\beta)]}{|X_n(jw)|Cos[\phi(w) - (\beta + T/2)w]}\right]^2 dw \tag{4.30}$$

We see that using equation (3.34), the Nyquist condition is expressed in the form of equations(3.16) where

$$|H[j(w_0 - w)]| = \frac{\sum_{i=1}^{m}(-1)^{i-1}A_i(w_0 - w)^{2(i-1)}}{|X_n[j(w_0 - w)]|Cos[\phi(w_0 - w) - (\beta + T/2)(w_0 - w)]} \quad (4.31)$$

$$|H[j(w_0 + w)]| = \frac{\sum_{i=1}^{m}(-1)^{i-1}A_i(w_0 + w)^{2(i-1)}}{|X_n[j(w_0 + w)]|Cos[\phi(w_0 + w) - (\beta + T/2)(w_0 + w)]} \quad (4.32)$$

and

$$|X_n(jw)| = \frac{|Q_n(jw)|}{|P(jw)|} \quad (4.33)$$

Substituting the respective terms in the equation (3.17), differentiating J w.r.t. $A_i's$ and equating the result to zero, we get the solution in the form of equation (3.43), where

$$X'_{(i,k)} = \int_{\beta-\delta 1}^{\beta+\delta 2} X4_i(t) \times X4_k(t).dt \quad (4.34)$$

$$X4_i(t) = \int_0^{2w_0} F'_i(w,t)dw \quad (4.35)$$

$$F'_i(w,t) = \frac{(-1)^{i-1}w^{2(i-1)}.Cos[w(t-\beta)]}{|X_n(jw)|\,Cos[\phi(w) - (\beta + T/2)w]} \quad (4.36)$$

$$Y'_{(i,r)} = V'_{(i,r)} + T'_{(i,r)} \tag{4.37}$$

$$V'_{(i,r)} = \frac{(-1)^{i-1}(w_0 - w)^{2(i-1)}}{|X_n[j(w_0 - w_r)]|\, Cos[\phi(w_0 - w_r) - (\beta + T/2)(w_0 - w_r)]} \tag{4.38}$$

$$T'_{(i,r)} = \frac{(-1)^{i-1}(w_0 + w)^{2(i-1)}}{|X_n[j(w_0 + w_r)]|\, Cos[\phi(w_0 + w_r) - (\beta + T/2)(w_0 + w_r)]} \tag{4.39}$$

$$Z'_{(i,k)} = \int_0^{2w_0} I'_i(w) \times I'_k(w).dw \tag{4.40}$$

$$I'_i(w) = \frac{(-1)^{i-1} w^{2(i-1)}}{|X_n(jw)| Cos[\phi(w) - \beta w]} \tag{4.41}$$

Also, we see that equation (3.38) can be expressed as

$$\sum_{i=1}^{m} A_i.Y'_{(i,r)} = C \tag{4.42}$$

where $r = 1, 2, ..., R.$ and $Y'_{(i,r)}$ is as defined in equation (4.37).

Equations (3.43) and (4.42) can be written in matrix form as shown in equation

(3.28). The coefficients $A_i's$ are found out by taking the first n terms of column vector A. Once $A_i's$ are determined, then one may use equations (4.27) and (4.28) to write

$$\frac{\sum_{i=1}^{m}(-1)^{i-1}A_{i.}w^{2(i-1)}}{|Q_n(jw)|Cos[\phi(w)-(\beta+T/2)w]} = \frac{\sum_{i=1}^{m1}(-1)^{i+1}B_{i.}w^{2i-1}}{|Q_n(jw)|Sin[\phi(w)-(\beta+T/2)w]} \tag{4.43}$$

or

$$\left[\sum_{i=1}^{m1}(-1)^{i+1}B_i w^{2i-1} - H_b(w)\right]^2 = \epsilon^2 \tag{4.44}$$

where

$$H_b(w) = \sum_{i=1}^{m}(-1)^{i-1}A_{i.}w^{2(i-1)}Tan[\phi(w)-(\beta+T/2)w]$$

Integrating equation (4.44) between 0 and $2w_0$ gives the total error within the full band of $2w_0$. To minimize this error, we differentiate with respect to $B_i's$ and set the result to zero. This gives

$$B_i = inv(M2) \times N2 \tag{4.45}$$

where

$$M2 = \frac{(-1)^{i+k+2}(2w_0)^{2i+2k-1}}{(2i+2k-1)} \tag{4.46}$$

and

$$N2 = \int_0^{2w_0} (-1)^{k+1} H_b(w) w^{2k-1} . dw \tag{4.47}$$

The finding of $B_i's$ completes the solution to determining the numerator coefficients of the data transmission filter.

Chapter 5

Results and Discussion

In this chapter, we present the various results obtained by using the proposed technique for the design of a data transmission filter. However, before giving a detailed investigation into the filter performance, we first present the procedure for choosing the design parameters in section 5.1. Section 5.2 deals with the results obtained for transfer functions with even powered numerator polynomial while section 5.3 deals with transfer functions with general numerator functions having both even and odd powers of w in the numerator. A comparison of the proposed designed technique is made with existing filter design methods for both even numerator and general numerator functions. Finally section 5.5 illustrates the realization of a 8^{th} filter using the method given in section 2.4.

5.1 Choice of Design Parameters

In this section, we summarize the procedure for choosing the various parameters in the design process to obtain the filter transfer function.

1. Select the degree n of the equidistant linear phase polynomial, the number m of unknown numerator coefficients, the number of precursor points (zero crossings before the main lobe) k_m, and the value of the location of the main lobe t_m. We further have to select the parameters α and β of the numerator polynomial defined in section (2.2.3). The parameter k_m is given by $k_m = \beta/T$ and need not be an integer [1]. Hence,

$$n\alpha = 2w_0 = \frac{2\pi\beta}{\beta}$$

and

$$\alpha\beta = \frac{2\pi k_m}{n}$$

The condition for a Hurwitz denominator is given as [1],

$$k_m < \frac{n}{4}$$

In our analysis of the filter design, k_m is chosen as $k_m = n/5$, leading to $\alpha\beta = 2\pi/5$ which guarantees the stability of the filters. The Nyquist frequency

w_0 is taken as 2π radians, the hence period of the impulse is $T = 0.5$ sec.

2. The value of the parameter α is then calculated using the relation $\alpha = 2\pi k_m/n\beta$. For $k_m = n/5$ and $\beta = n/10$, $\alpha = 4\pi/n$.

3. In order to maximize the energy in the main lobe of the impulse response, we make $\sigma = 1$ so that the selected interval for energy maximization is $(-T, T)$.

4. The least mean square approximation along with the Nyquist criteria then gives the unknown numerator coefficients, which completely determines the filter transfer function.

5.2 Results for Even Numerator Functions

This section gives the results for transmission filters designed with even powered functions of w in the numerator. In this case, the phase of the filter is the reciprocal of that of the linear phase polynomial.

The design was performed for various values of λ and the filter performance parameters defined earlier were evaluated. Table (5.1) and table (5.2) illustrate the filter performance for n=even and n=odd respectively for $\lambda = 0.985$, having an excess bandwidth $\gamma = 1$. Figures (5.1-5.4) show the time, phase and frequency responses of a 14^{th} order transmission filter of the proposed design. Table (5.3) gives the performance for transmission filter characteristics for λ=0.995. Figures (5.5-5.8)

show the respective time, phase and frequency response of this filter for n=14.

We observe that the performance of the filter improves gradually with increase in the filter order n. Smaller sampling errors were achieved for higher order filters because of the reduction in the linear phase error. Also, using higher filter orders result in closer approximation to the ideal filter characteristics which is evident from higher attenuations and smaller sidelobes of the impulse response.

order n	8	10	12	14
k_m-β	1.6-0.8	2-1	2.1-1.2	2.8-1.4
λ	0.985	0.985	0.985	0.985
Min. attenuation in dB	46.3	50.8	53.1	59.87
Max. overshoot in dB	0.0	0.0	0.0	0.0
Side Lobe in %	3.0	2.3	2.12	2.0
Sampling Error	2.91 E-5	1.64 E-5	8.36 E-6	3.42 E-6
Max. Phase Deviation	6.3 E-2	4.2 E-2	3.2 E-2	2.2 E-2

Table 5.1: Filter performance for Model I functions, λ=0.985 and n even

order n	9	11	13	15
k_m-β	1.8-0.9	2.2-1.1	2.6-1.3	3.0-1.5
λ	0.985	0.985	0.985	0.985
Min. attenuation in dB	50.1	52.8	56.5	61.2
Max. overshoot in dB	0.0	0.0	0.0	0.0
Side Lobe in %	2.8	2.2	2.08	2.0
Sampling Error	2.83 E-5	9.15 E-6	7.91 E-6	2.28 E-6
Max. Phase Deviation	5.4 E-2	3.9 E-2	2.8 E-2	2.05 E-2

Table 5.2: Filter performance for Model I functions, λ=0.985 and n odd.

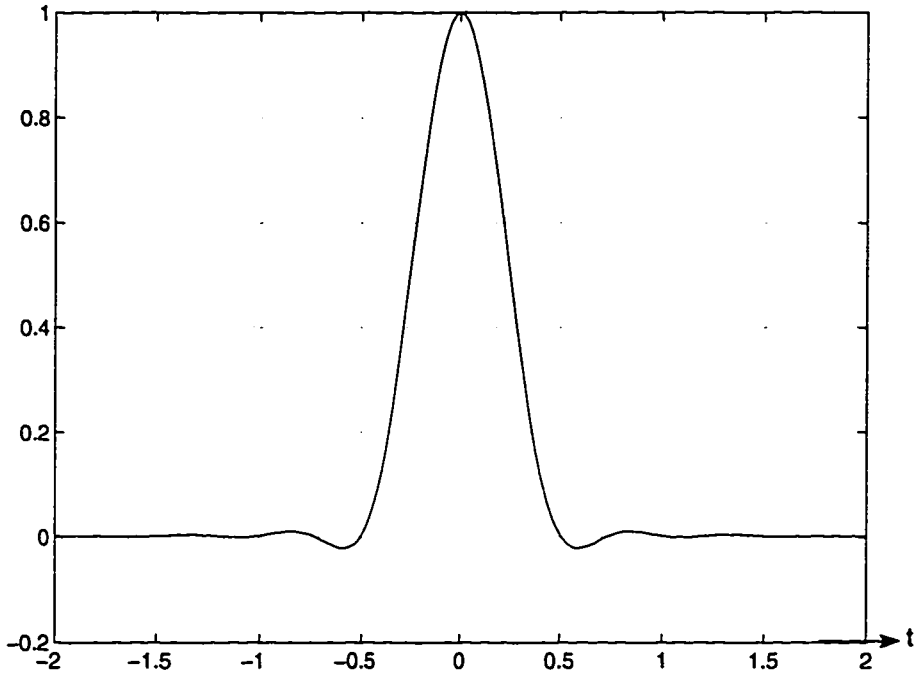

Figure 5.1: Normalized Impulse Response for Model I, n=14 and λ=0.985

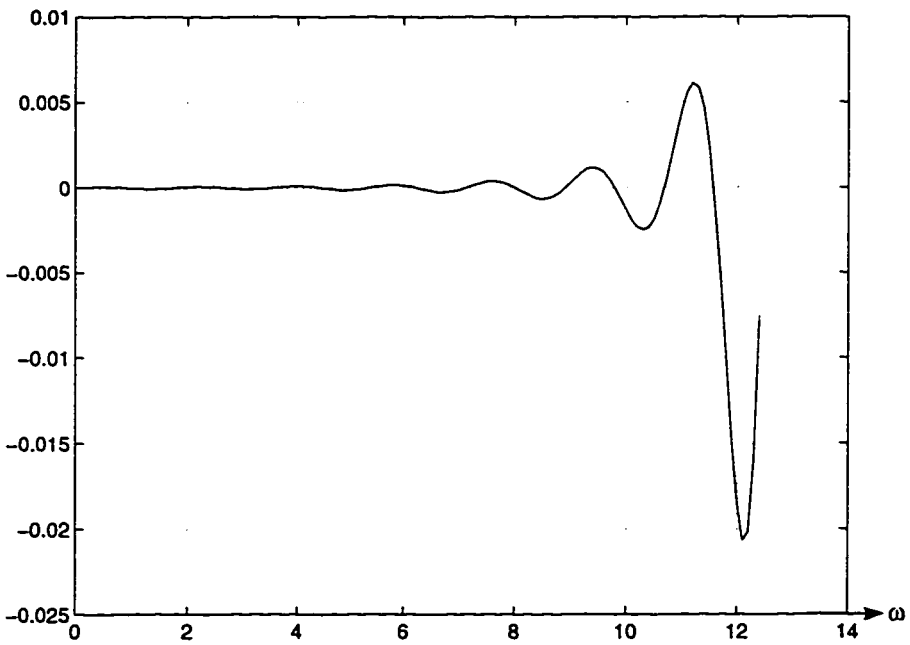

Figure 5.2: Linear Phase Error for Model I, n=14 and λ=0.985

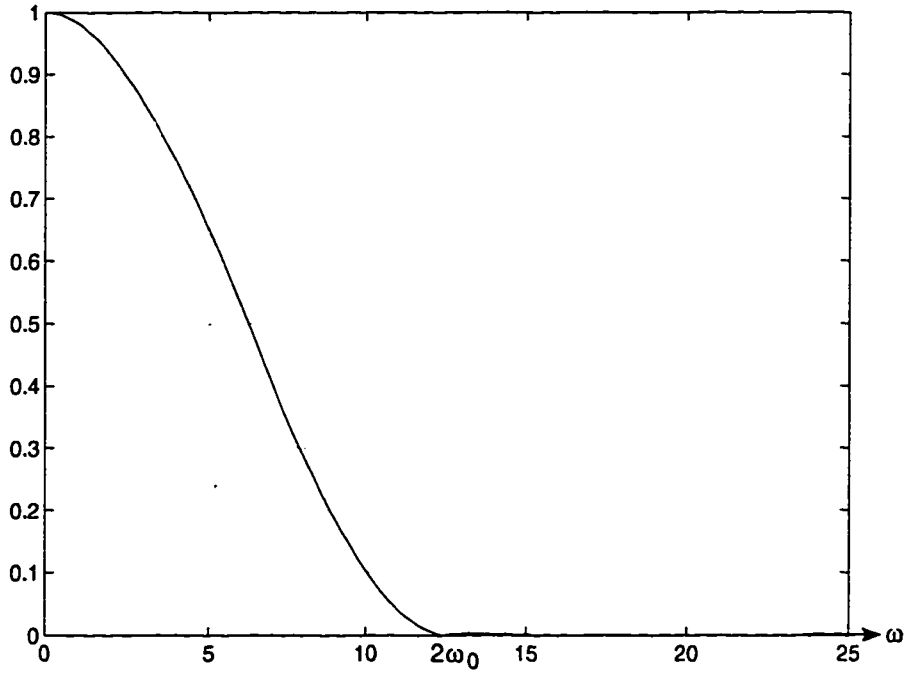

Figure 5.3: Normalized Frequency Response for Model I, n=14 and λ=0.985

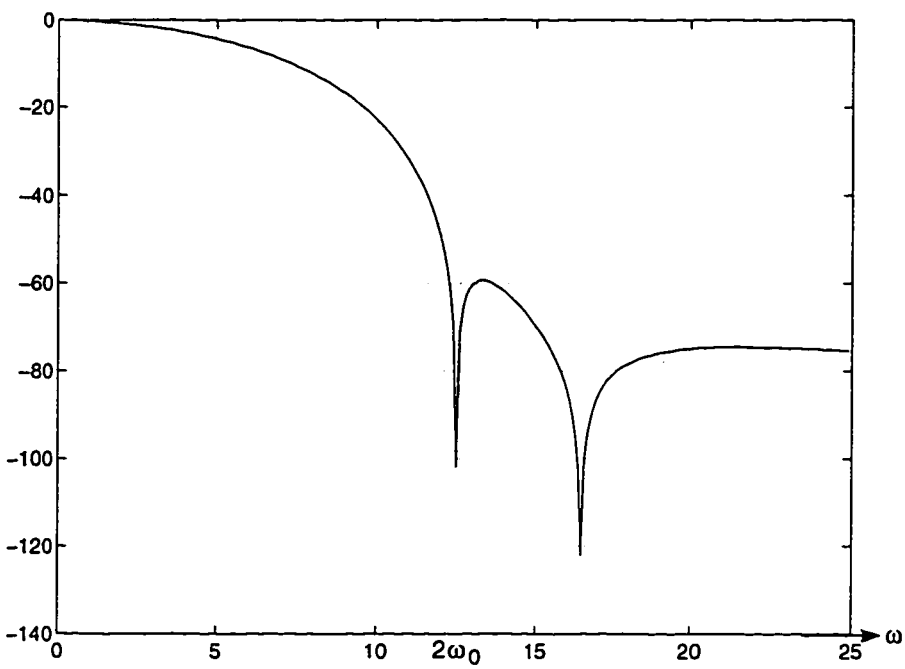

Figure 5.4: Frequency Response in dB for Model I, n=14 and λ=0.985

order n	8	10	12	14
k_m-β	1.6-0.8	2-1	2.1-1.2	2.8-1.4
λ	0.995	0.995	0.995	0.995
Min. attenuation in dB at $2w_0$	33.8	34.2	34.5	37.1
Max. overshoot in dB	0.0	0.0	0.0	0.0
Side Lobe in %	0.69	0.64	0.634	0.628
Sampling Error	2.64 E-5	7.41 E-6	6.59 E-6	5.81 E-6
Max. Phase Deviation	6.3 E-2	4.2 E-2	3.2 E-2	2.2 E-2

Table 5.3: Filter performance for Model I functions for $\lambda = 0.995$

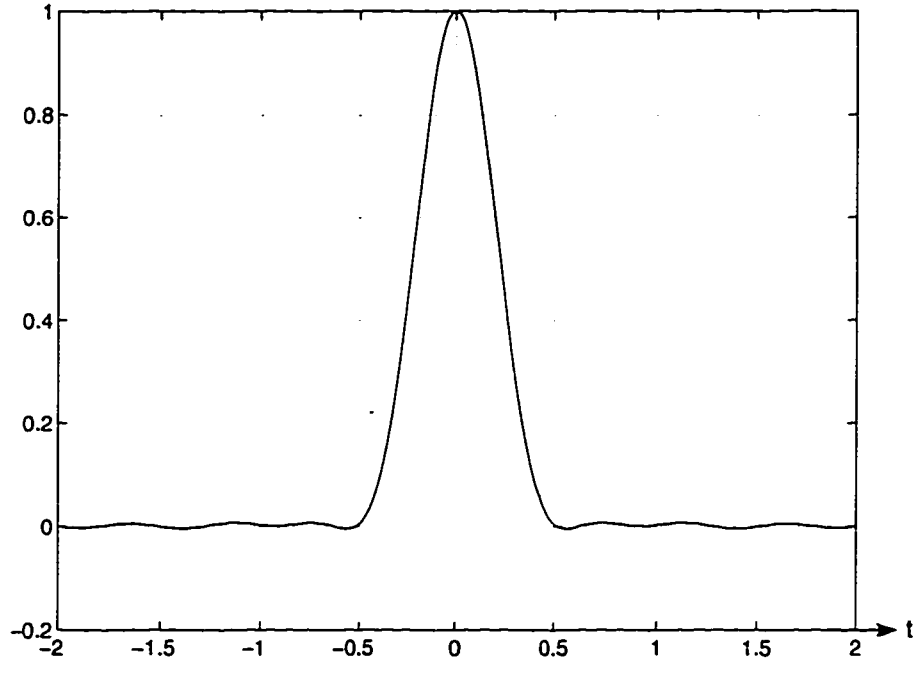

Figure 5.5: Normalized Impulse Response for Model I, n=14 and λ=.995

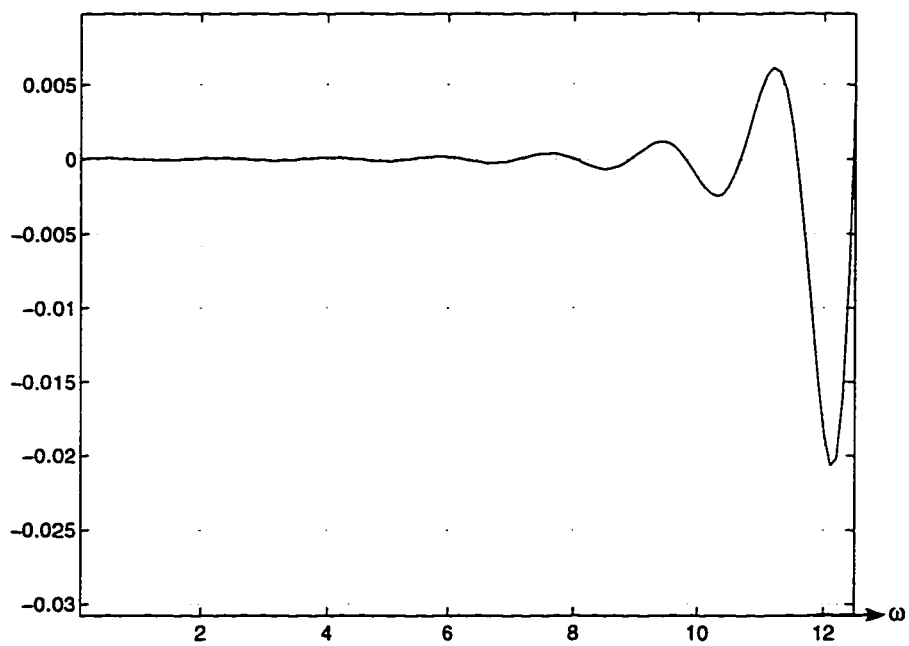

Figure 5.6: Linear Phase Error for Model I, n=14 and λ=.995

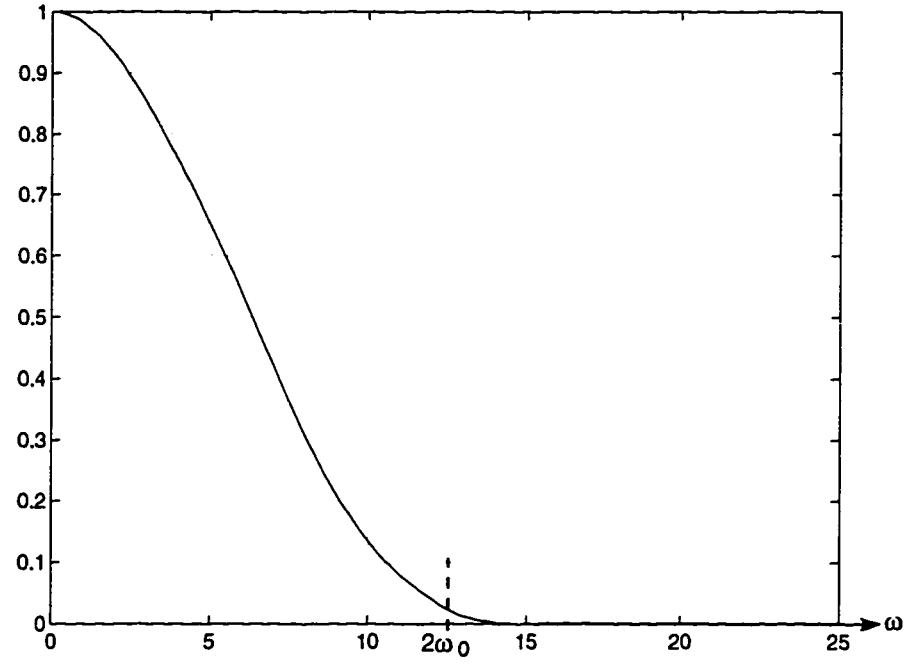

Figure 5.7: Normalized Frequency Response for Model I, n=14 and λ=.995

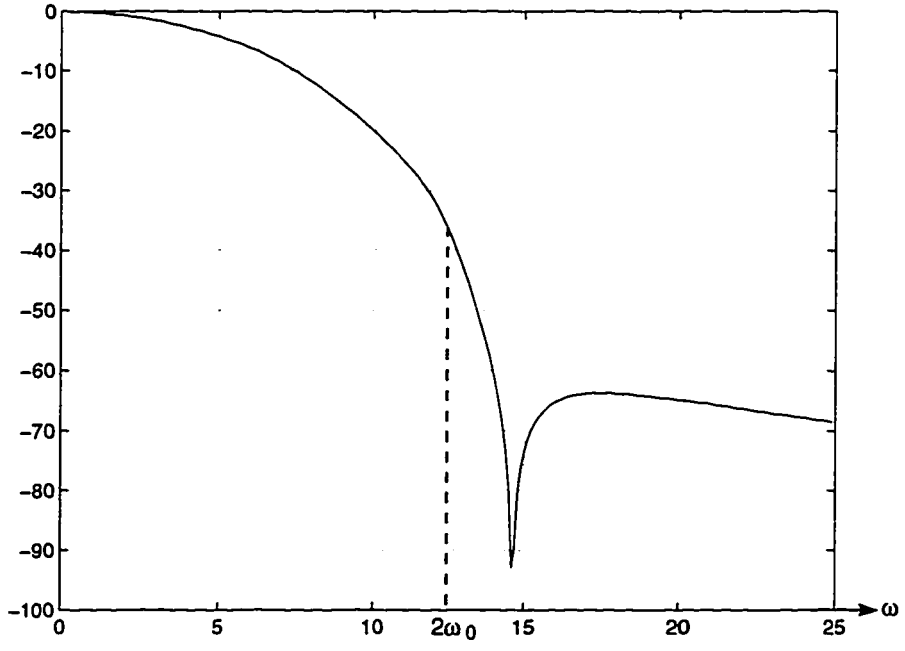

Figure 5.8: Frequency Response in dB for Model I, n=14 and λ=.995

5.3 Results for General Numerator Functions

This section gives the results for transmission filters designed with general numerator functions having both even and odd powers of w in the numerator using the theory covered in chapter 4.

Table (5.4) and table (5.5) give the designed filter performance measure for n=even and n=odd respectively for an equivalent raised cosine filter with excess bandwidth $\gamma = 1$. Figures (5.9-5.12) show the time, phase and frequency responses of a 14^{th} order transmission filter of such kind. Table (5.6) gives the filter performance for λ=0.995. Figures (5.13-5.16) show the time, phase and frequency response of this filter for n=14;

We notice from the results that for Model II, there is considerable reduction in the maximum phase deviation of the filter response when compared to the even numerator transfer functions. The decrease in the maximum linear phase error is at the expense of greater phase error at lower frequencies. This model also achieved higher attenuations. However, one has to consider the increased complexity of the circuit for general numerator functions when considering the improvements in response.

order n	8	10	12	14
k_m-β	1.6-0.8	2-1	2.1-1.2	2.8-1.4
λ	0.985	0.985	0.985	0.985
Min. attenuation in dB	50.8	53.2	59.28	62.54
Max. overshoot in dB	0.0	0.0	0.0	0.0
Side Lobe in %	2.8	2.23	2.18	2.05
Sampling Error	1.61 E-5	9.17 E-6	6.81 E-6	2.86 E-6
Max. Phase Deviation	4.8 E-2	2.8 E-2	1.9 E-2	8.5 E-3

Table 5.4: Filter performance for Model II functions, λ=0.985 and n even

order n	9	11	13	15
k_m-β	1.8-0.9	2.2-1.1	2.6-1.3	3.0-1.5
λ	0.985	0.985	0.985	0.985
Min. attenuation in dB	52.16	57.1	60.23	62.7
Max. overshoot in dB	0.0	0.0	0.0	0.0
Side Lobe in %	2.31	2.2	2.12	2.0
Sampling Error	1.22 E-5	6.81 E-6	4.52 E-6	2.13 E-6
Max. Phase Deviation	3.5 E-2	2.3 E-2	1.14 E-2	7.2 E-3

Table 5.5: Filter performance for Model II functions, λ=0.985 and n odd

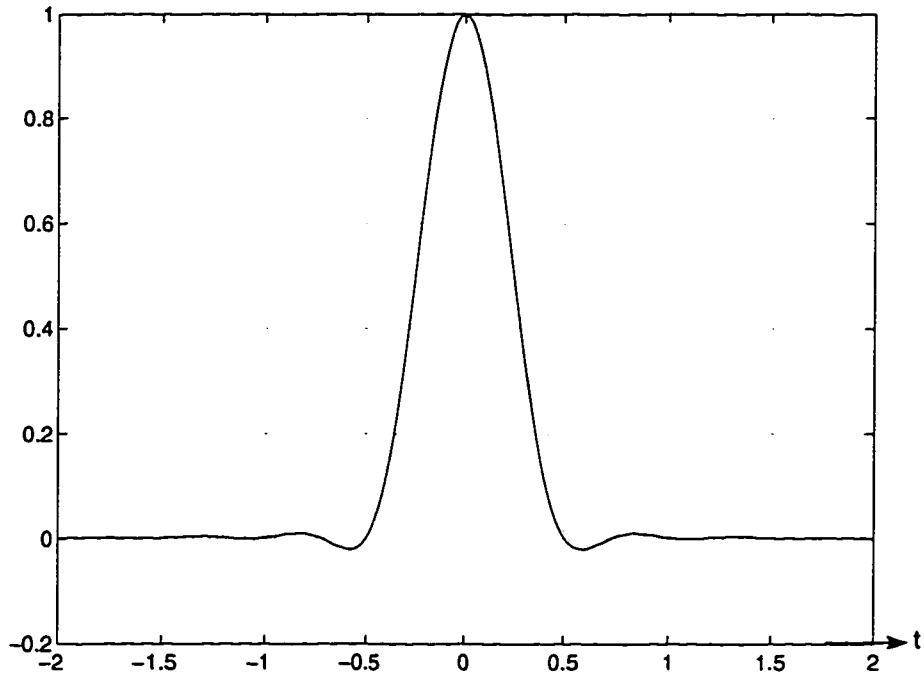

Figure 5.9: Normalized Impulse Response for Model II, n=14 and λ=0.985

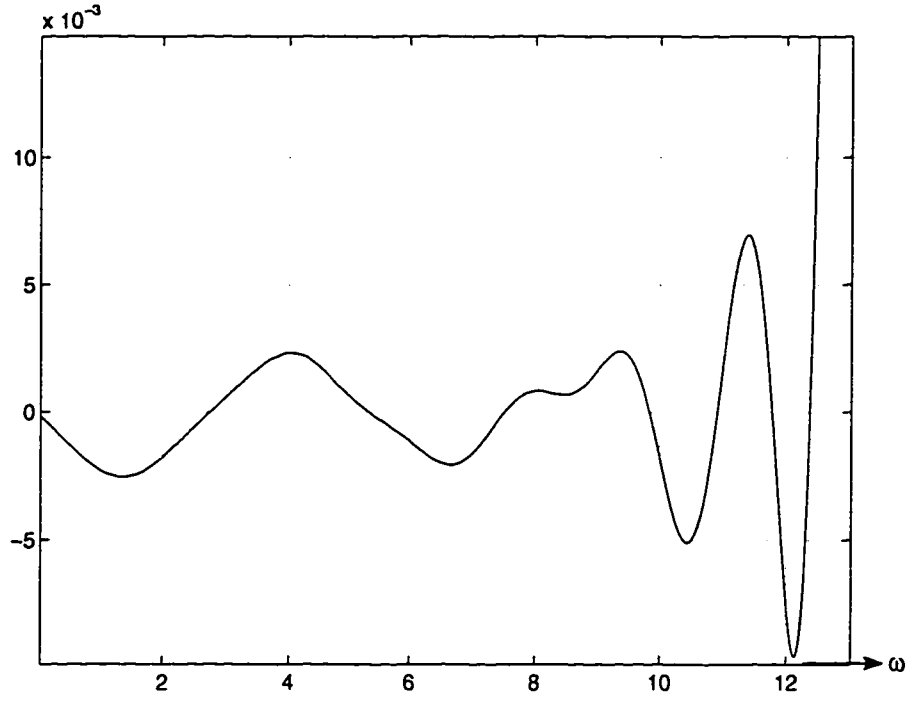

Figure 5.10: Linear Phase Error for Model II, n=14 and λ=0.985

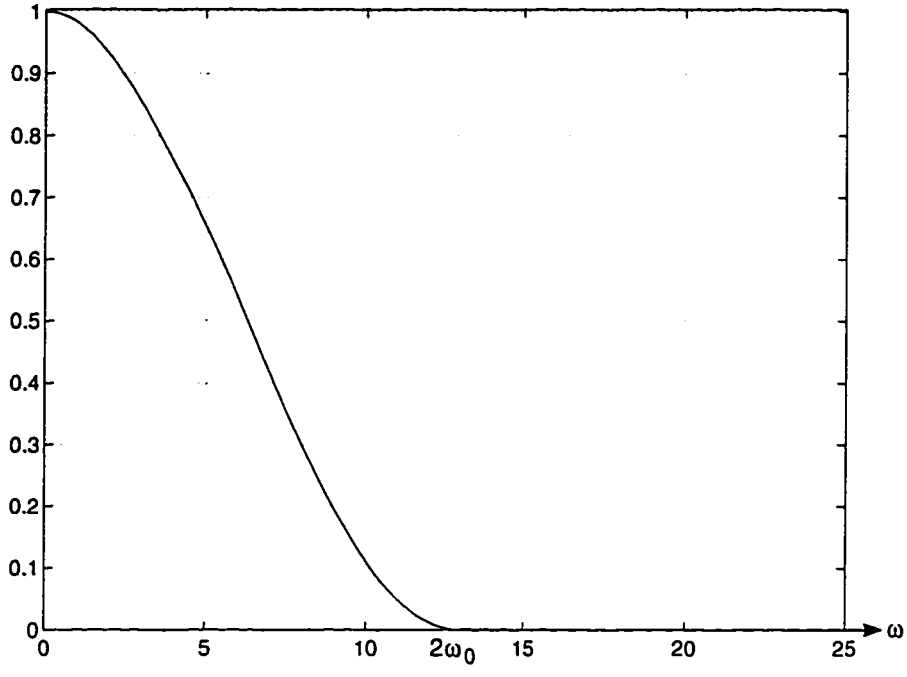

Figure 5.11: Normalized Frequency Response for Model II, n=14 and λ=0.985

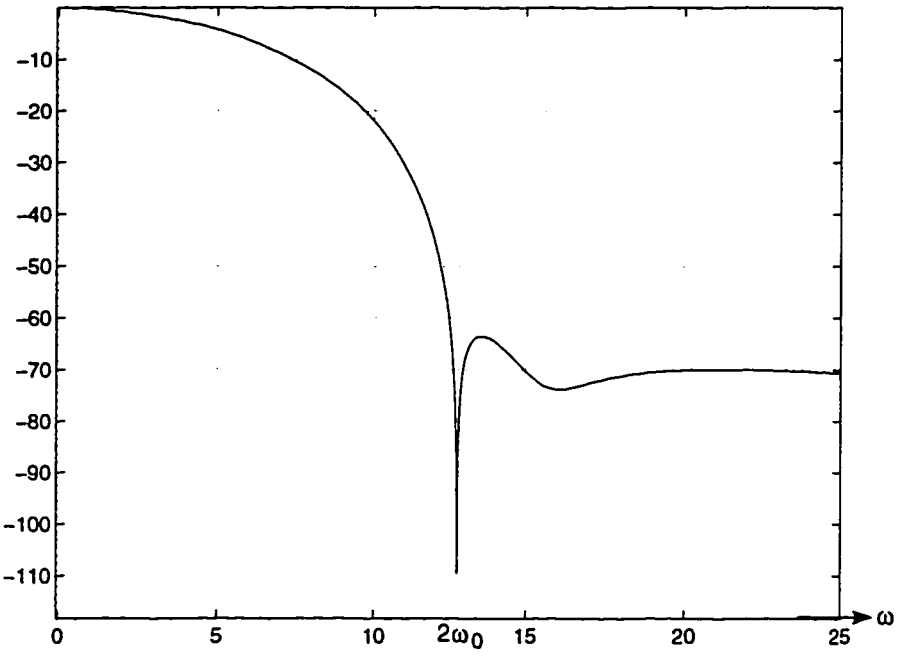

Figure 5.12: Frequency Response in dB for Model II, n=14 and λ=0.985

order n	8	10	12	14
k_m-β	1.6-0.8	2-1	2.1-1.2	2.8-1.4
λ	0.995	0.995	0.995	0.995
Min. attenuation in dB at $2w_0$	33.6	33.9	34.2	34.3
Max. overshoot in dB	0.0	0.0	0.0	0.0
Side Lobe in %	0.71	0.65	0.64	0.62
Sampling Error	7.21 E-6	5.68 E-6	5.14 E-6	3.19 E-6
Max. Phase Deviation	4.7 E-2	2.1 E-2	1.4 E-2	7.32 E-3

Table 5.6: Filter performance for Model II with λ=0.995

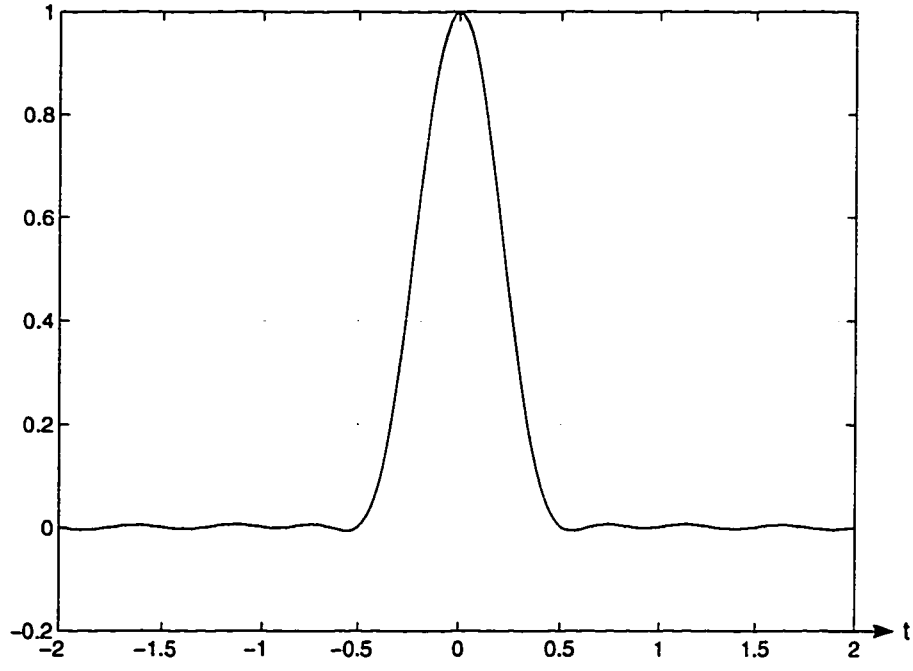

Figure 5.13: Normalized Impulse Response for Model II, n=14 and λ=0.995

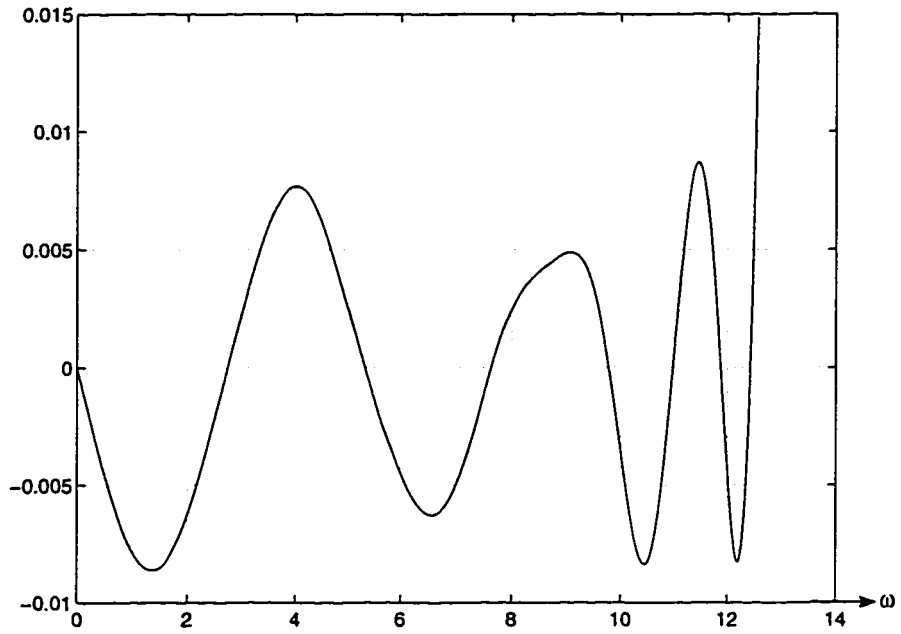

Figure 5.14: Linear Phase Error for Model II, n=14 and λ=0.995

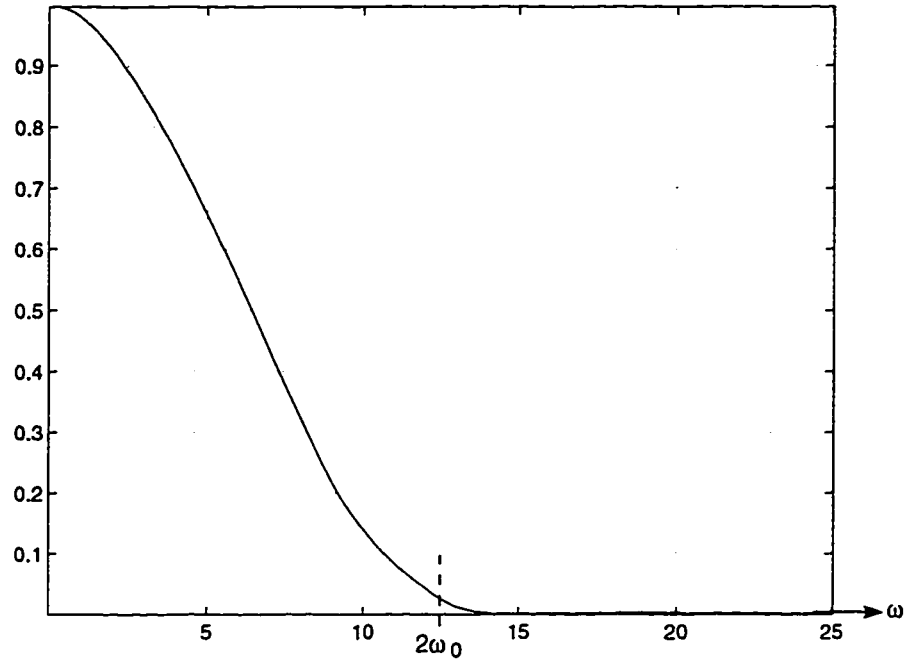

Figure 5.15: Normalized Frequency Response for Model II, n=14 and λ=0.995

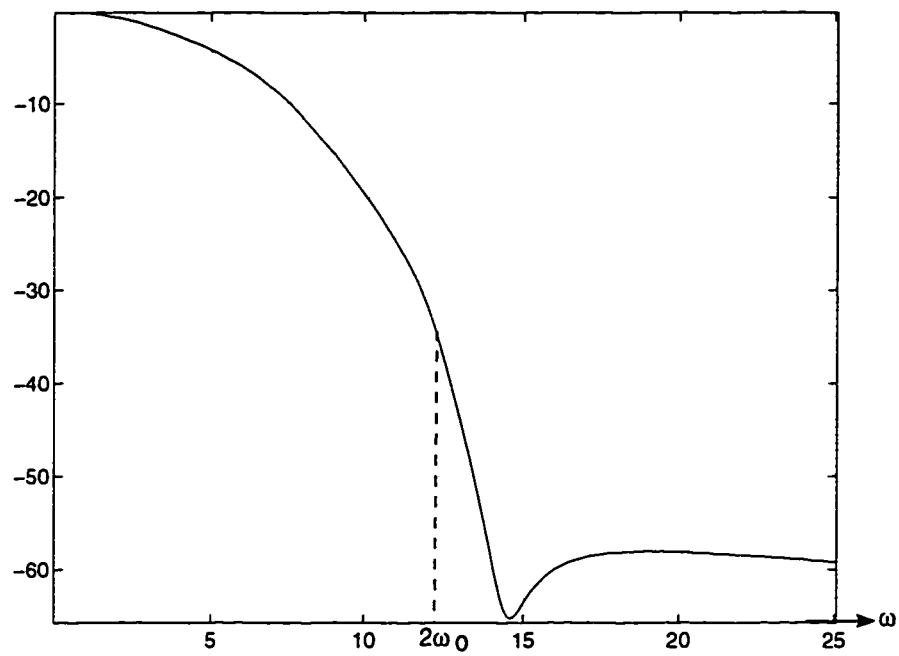

Figure 5.16: Frequency Response in dB for Model II, n=14 and λ=0.995

5.4 Comparison

In this subsection, we compare the results obtained by using the proposed design technique with the previously published results. This is done by defining a common criteria which is the bandwidth limitation. The results of Model I design are compared with the results published in [1] whereas the results of Model II are compared to that published in [11]. The comparisons are based on simulations performed in MATLAB on the design theory proposed in [1] and [11] respectively.

5.4.1 Model I Comparison

The results of the proposed work of Model I are compared with that of [1] by defining a common bandwidth constraint. The bandwidth was taken as 1.75 w_0 and is defined such that the maximum frequency beyond which the gain is less than -40 dB. The results were compared for order of the filter varying form 8 to 14. The comparison is tabulated in table (5.7). We see that the size of the side lobes of the proposed work are relatively smaller when compared to that of [1]. The sampling errors obtained are comparable to that of [1]. The proposed design gives smaller sampling error for lower order filters but the results tend to get inferior to that of [1] at higher orders.

order n	8		10		12		14	
α, β	1.57, 0.8		1.25, 1.0		1.047, 1.2		0.89, 1.4	
	Ref [1]	This Work	Ref [1]	This Work	Ref [1]	This Work	Ref [1]	This Work
Slope at w_0	-0.145	-0.126	-0.142	-0.123	-0.138	-0.125	-0.125	-0.126
Max. Overshoot in dB	0.0	0.0	0.0	0.0	0.0	0.0	0.0	0.0
Side lobe in %	3.61	2.73	3.49	2.62	3.34	2.50	3.14	2.39
Sampling Error	8.49 E-4	5.12 E-4	5.98 E-4	3.56 E-4	2.57 E-4	2.32 E-4	7.13 E-5	9.21 E-5

Table 5.7: Comparison with previous published results using Model I

5.4.2 Model II Comparison

The result of Model II functions are compared with that of [11] for the case of 100% excess bandwidth. The results of the two methods are compared with respect to the out of band attenuation, sampling errors, size of the side lobes and the reduction in the linear phase deviation. Simulations were performed in MATLAB and the results thus obtained are tabulated in table (5.8).

We see that the performance of the proposed work shows higher attenuations, much smaller side lobes and comparable sampling errors for all filter orders. However the reduction in the maximum phase deviation has not been as considerable as compared to data published in [11].

order n α, β	8 1.57, 0.8		10 1.25, 1.0		12 1.047, 1.2		14 0.89, 1.4	
	Ref [11] γ=1	This Work λ=.985	Ref [11] γ=1	This Work λ=.985	Ref [11] γ=1	This Work λ=.985	Ref [11] γ=1	This Work λ=.985
Min. Attn. in dB	40.1	50.8	44.0	53.2	48.0	59.28	51.6	63.54
Side lobe in %	3.2	2.8	2.7	2.23	2.84	2.18	2.7	2.05
Sampling Error	4.5 E-5	1.61 E-5	2.48 E-5	9.17 E-6	1.96 E-5	6.81 E-6	3.8 E-6	2.86 E-6
Max. Phase Deviation	3.7 E-2	4.8 E-2	2.0 E-2	2.8 E-2	1.3 E-2	1.9 E-2	6.4 E-3	8.5 E-3

Table 5.8: Comparison with previous published results using Model II

5.4.3 Model I Vs Model II Comparison

In section (2.4), it was shown that the transfer functions of the same order of Model I and Model II require different number of elements for their realization. Therefore a comparison between the two studied models i.e, Model I and Model II will be fair only if the number of elements involved in both the realizations are equal. For this purpose, the comparison of the evaluation parameters is done by taking n=14 for Model I function and n=8 for Model II function. The results are tabulated in table (5.9).

We see that for the same value of λ=0.985, the performance of Model I functions are better in both the frequency and time domain characteristics when compared to Model II functions. Therefore, eventhough for the same order n, the performance of Model II seems better, the performance of Model I is better with equal number of components used in network realization. Hence Model I functions are preferred.

	Model I (n=14)	Model II (n=7)
λ	0.985	0.985
Min. attenuation in dB	59.87	50.1
Max. overshoot in dB	0.0	0.0
Side Lobe in %	2.0	2.85
Sampling Error	3.42 E-6	4.83 E-5
Max. Phase Deviation	2.2 E-2	5.16 E-2

Table 5.9: Model I Vs Model II comparison

5.5 Realization

An 8^{th} order circuit for even numerator functions designed using the proposed technique is realized using the procedure in section (2.4). The designed filter transfer function is

$$H_8(s) = \frac{325.5-1.08s^2-0.0201s^4+1.93\,10^{-5}s^6}{325.5+257.6s+98.9s^2+22.7s^3+3.83s^4+0.421s^5+3.97\,10^{-2}s^6+1.97\,10^{-3}s^7+1.07\,10^{-4}s^8}$$

The impedance $Z(s)$ of the network to be synthesized for the above transfer function is found using equations (2.35) and (2.36) as

$$Z(s) = \frac{680609+613171s+282352s^2+68413s^3+12939s^4+1434s^5+149.8s^6+7.24s^7+0.448s^8}{680609+464093s+131241s^2+26517s^3+3078.2s^4+327.1s^5+16.2s^6+s^7}$$

The above impedance has a pole at $s = \infty$, which is extracted as a series inductor of the value

$$L_1 = \lim_{s\to\infty}\left\{\frac{Z(s)}{s}\right\}$$

The remainder impedance, $Z_1(s)$ after the pole extraction is given by

$$Z_1(s) = Z(s) - L_1 s$$

and is found out as

$$Z_1(s) = \frac{680609+308621s+74685s^2+9687s^3+1073s^4+56.09s^5+3.46s^6}{680609+464093s+131241s^2+26517s^3+3078s^4+327.1s^5+16.17s^6+s^7}$$

We see that $Y_1(s) = 1/Z_1(s)$ has a pole at $s = \infty$, which is extracted as a shunt capacitor of the value

$$C_1 = \lim_{s \to \infty} \left\{ \frac{Y_(s)}{s} \right\}$$

The remainder admittance $Y_2(s)$ is given by

$$Y_2(s) = Y_1(s) - C_1 s$$

and found out as

$$Y_2(s) = \frac{196261+88994s+21536s^2+2793s^3+309.4s^4+16.17s^5+s^6}{196261+77232s+12182s^2+1436s^3+82.15s^4+5.0985s^5+0.00135s^6}$$

Therefore,

$$Z_2(s) = \frac{196261+77232s+12182s^2+1436s^3+82.15s^4+5.09s^5+0.000135s^6}{196261+88994s+21536s^2+2793s^3+309.4s^4+16.17*s^5+s^6}$$

which is minimum reactance and minimum susceptance.

The zeros of transmission of the polynomial $Z_2(s)$ are found out as outlined in section (2.4.2) as

$$m_1 m_2 - n_1 n_2 = (s^2 + 146.41)^2 (s^2 - 1078.47)^2 (s^2 - 107.58)^2$$

Therefore, there exists a double order zero on the jw axis at $s = \pm i12.1$ which is realized by a Brune Section and two double order zeros on the real axis at $s = \pm 32.84$ and $s = \pm 10.82$ respectively which may be realized by two C sections. The complete network designed for the Nyquist frequency of 10 MHz and a terminating resistance

of 100 Ohms is shown in figure (5.17). The circuit can be verified by the PSPICE program given in Appendix A. The element values thus obtained for the circuit shown in figure (5.17) are

$$L_1 = 0.044747\,mH$$

$$L_2 = 0.025478\,mH$$

$$L_3 = 4.005891\,\mu H$$

$$L_4 = 13.45215\,\mu H$$

$$L_5 = 0.033678\,\mu H$$

$$L_6 = 8.409491\,\mu H$$

$$L_7 = 2.886552\,\mu H$$

$$M_1 = 10.10261\,\mu H$$

$$M_2 = -0.67303\,\mu H$$

$$M_3 = -4.9269\,\mu H$$

$$C_1 = 2.883613\,nF$$

$$C_2 = 682.1312\,pF$$

$$C_3 = 1.377225\,nF$$

$$C_4 = 1.865853\,nF$$

$$R_L = 100\ Ohms$$

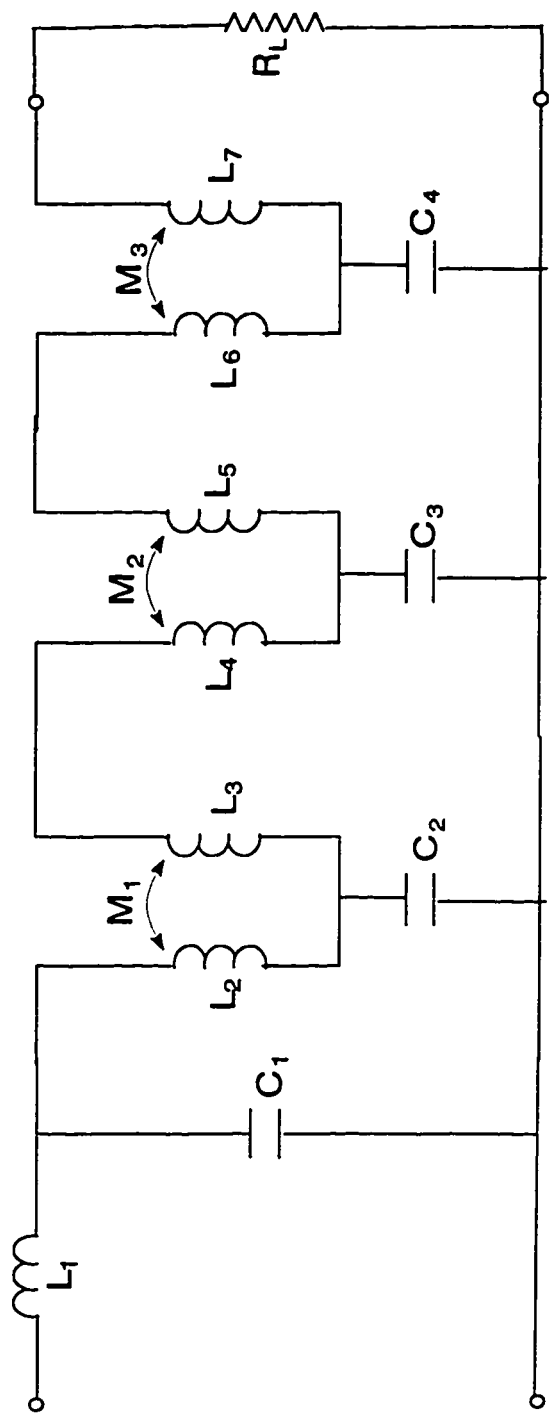

Figure 5.17: Network of an 8^{th} order designed function

Chapter 6

Conclusion and Recommendations

A linear phase, Nyquist data transmission filter is designed where the energy in the main lobe of the impulse response is optimized to produce rapidly decaying pulses in the time domain. The design has been implemented for the filter orders ranging from 8 to 15 using computer programs in MATLAB. The results were obtained for different values of the energy ratio parameter λ for the two filter models. The first model termed as Model I is used to optimize the magnitude of the filter transfer function while the second model termed as Model II, is used to optimize the magnitude and phase of the filter simultaneously.

6.1 Conclusion

Based on the results presented in Chapter 5, the following conclusions can be made.

1. For constant values of energy ratio parameter λ, we see that, as the degree of the filter is increased, the time response of the filter improves. This results in smaller first sidelobe size of the impulse response. The time response of the filter becomes negligible after one or two zero crossings beyond the main lobe. This is a major advantage as it reduces the error due to jittering and non-ideal sampling and hence improving the bit error rate (BER).

2. The sampling error of the filter decreases with increase in filter order. Sampling errors of the order of 10^{-6} were achieved, which are quite negligible. This further improves the system BER.

3. In the frequency domain, it is noticed that the attenuation beyond $2w_0$ increases as the filter order is increased. The attenuations achieved are in the range of 60 dB which guarantee complete elimination of neighboring frequency interference.

4. The maximum linear phase error in the range of $[0,2w_0]$ decreases with increase in filter order. Smaller phase errors were achieved using the general polynomials with both even and odd powers of w in the numerator. However,

this is achieved at the cost of network complexity.

5. A trade-off between frequency domain characteristics and the time domain characteristics is noticed with the variation of the energy ratio parameter λ. As λ is increased, the sidelobes of the impulse response of the filter decreases to very low values. However, for $\lambda > 0.985$, the frequency spectrum of the filter spreads beyond $2w_0$ and smaller attenuations of the order of 30-35 dB at the cutoff frequency are evident.

6. It is noticed that for equal number of elements used in the network realization, the performance of Model I function is superior in all aspects when compared to Model II function. Therefore the use of Model II function is not recommended and one should opt for Model I function which is less complex and gives superior performance characteristics.

Finally, the design of a Nyquist filter based on a pulse rather than impulse input is tackled. This is very important since it represents the reality of applications. It is found that the results of this work are comparable to that of [1] and [11] with better time response decay which makes the design very attractive for industrial use. The method therefore, presents a useful technique to design a Nyquist filter particularly useful to combat intersymbol interference and jitter effects.

6.2 Recommendations

At the end of the study, the following recommendations may set a good basis for future research.

1. The proposed design technique may be extended to the design of digital filter transfer functions for data transmission using known methods such as the impulse invariance method.

2. If the filter specifications are given in frequency domain, one may look into incorporating the specific bandwidth or the slope of the frequency response at w_0 in the design. This may provide better frequency selectivity.

3. The design of linear phase bandpass filter is a challenging problem. However, keeping the phase linear as one performs frequency transformations from low pass to bandpass requires some modification to the linear phase polynomial. This is a good research problem for further study.

Bibliography

[1] Baher H. and Beneat J. Design of analog and digital data transmission filters. *IEEE Transactions on Circuit Theory*, 40:449–460, 1993.

[2] Gibby A.J. and Smith J.W. Some extentions of Nyquist telegraph transmission theory . *Bell Syst. Tech. Journal*, 44:1487–1506, 1965.

[3] Patrick R. Trischitta and Eve L. Varma. *Jitter in Transmission Systems.* Norwood: Artech House, 1989.

[4] Baher H. *Synthesis of Electrical Networks.* NewYork: Wiley, 1984.

[5] Rhodes J.D. *Theory of Electrial Filters.* New York: Wiley, 1976.

[6] Nyquist H. Certain topics in telegraph transmission theory. *IEEE Transactions on AIEE*, 47:617–644, 1928.

[7] Nader S.E and Lind L.F. Optimal data transmission filters . *IEEE Transactions on Circuits and Systems*, 26:36–45, 1979.

[8] John Proakis G. *Digital Communication.* NewYork: McGraw-Hill, 1989.

[9] M.S.Ulstad. Time domain approximations and an active network transfer functions derived from ideal filters . *IEEE transactions on Circuit Theory*, 15:205–211, 1968.

[10] Hassan E.E. Time domain energy maximization of the Nyquist pulse. *International Journal of Electronics*, 76(2):213–219, 1994.

[11] Hassan E.E. and Ragheb H. On the design of linear phase Nyquist filter. *IEE Transactions on Circuits and Systems*, 1996.

[12] Scalan J. O. Pulses satisfying Nyquist criterion. *Electronic Letters*, 28:50–52, 1992.

[13] Spauling D.A. Synthesis of pulse-shaping networks in the time domain. *Bell Syst. Tech. Journal*, 48:2425–2444, 1969.

[14] Tugbay N. and Panayiri E. Energy optimization of band limited Nyquist signals in the time domain. *IEEE transactions on communications*, 35:427–434, 1987.

[15] Scalan O.J. and J.D.Rhodes. Unified theory of cascade synthesis . *Proceedings of IEEE*, 4:665–670, 1970.

[16] Shanmugam K. *Digital and Analog Communication Systems.* NewYork: Wiley, 1979.

[17] Bissell C. and A. Chapman. *Digital Signal Transmission.* Cambridge: Cambridge University Press, 1992.

Appendix A
PSPICE Program

```
* THIS IS THE PSPICE SIMULATION OF THE DESIGNED NETWORK
* INPUT PULSE
*VIN 1 0 AC 1m
VIN 1 0 PULSE(0 1E+2 0 0 0 0.5S 10S)
* RESISTORS
RI 1 2 100
RL 9 0 100
* INDUCTORS
L1 2 3 0.044747 mH
L2 3 4 0.025478 mH
L3 5 4 4.00589 UH
L4 5 6 13.45215 UH
L5 6 7 0.033678 UH
L6 7 8 8.40949 UH
L7 8 9 2.88655 UH
* MUTUAL INDUCTANCES
K23 L2 L3 10.1026 UH
K45 L4 L5 -0.67303 UH
K67 L6 L7 -4.92691 UH
*CAPACITORS
C1 3 0 2.883614 nF
C2 4 0 682.1312 pF
C3 6 0 1.37722 nF
C4 8 0 1.86585 nF
*TRANSIENT TIME RESPONSE
.TRAN .05 10
.PRINT TRAN V(9)
*FREQUENCY RESPONSE
*.AC LIN 100 .001HZ 4HZ
*.PRINT AC VM(9) VP(9)
*.PROBE
* END STATEMENT
.END
```

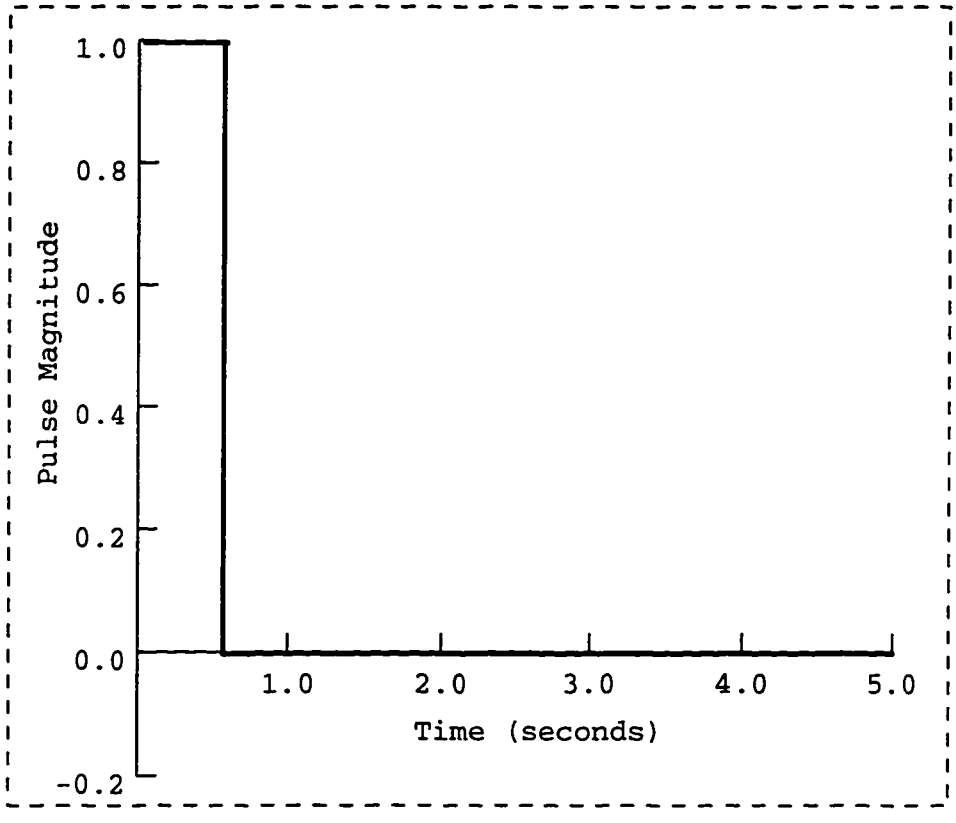

Figure .1: Pulse Input to the Network of Figure (5.17)

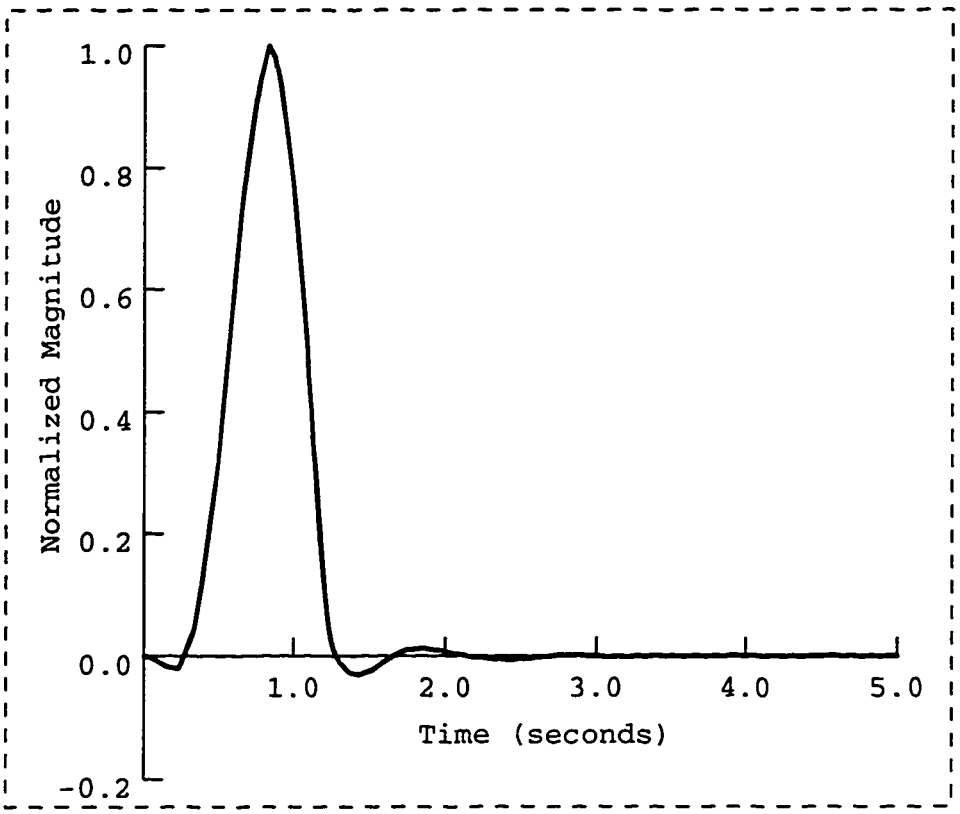

Figure .2: Pulse response of the Network of Figure (5.17)